Surface plasmaritons: Wave-mechanical and second-quantized theories

Jesper Jung and Ole Keller*

Institute of Physics, Aalborg University, Skjernvej 4A, DK-9220 Aalborg Øst, Denmark

(Received 5 February 2022; accepted 15 August 2022; published 8 September 2022)

In the wake of recently established quantum theories for bulk and surface plasmons, and for bulk plasmaritons [Jung and Keller, Phys. Rev. A **103**, 063501 (2021); **104**, 053508 (2021)] wave-mechanical and second-quantized (QED) theories for surface plasmaritons are developed. Our photon wave-mechanical theory is based on the covariant four-potential in the Lorenz gauge, where dynamical equations for surface plasmariton quantum particles consisting of scalar (S), longitudinal (L), and transverse ($T1$, $T2$) photons and driven by a surface current density sheet are obtained. The second quantized QED theory of surface plasmaritons is formulated on the basis of the Heisenberg equations of motion for the contravariant four-potential annihilation operators. The connection of the surface plasmariton quantum theory to the quasiparticle picture of bulk plasmaritons is elucidated by studying the T-photon exponential decay lengths appearing in the description. The shortest decay length (equal on both sides of the surface) characterizes the one-dimensional spatial confinement of the T-photon source. Starting from a reexamination (and correction) of the dynamic boundary conditions for a flat jellium-vacuum interface carrying a surface current density, the dispersion relation for surface plasmaritons is obtained. The explicit form of the dispersion relation is derived upon a study of the local field in the selvedge region of the boundary. Fundamental aspects of the dispersion relation are pointed out, modeling the electron dynamics by the microscopic electrodynamics of a quantum well. Remarks on (i) our covariant surface plasmariton quantum theory seen in a broader perspective, (ii) suggestions for applications of the theory, and (iii) a comparison of the key ingredients in our trio of papers on plasmon and plasmariton quantum physics are presented.

DOI: 10.1103/PhysRevA.106.033503

I. INTRODUCTION

A surface polariton, roughly speaking, is a p-polarized electromagnetic wave that propagates in a wavelike fashion along the (plane) surface of a solid medium or along the interface between two media. The strength of the electromagnetic field associated with the wave decays exponentially as one moves away from the interface into either medium. In the special case (studied in this paper) where the surface separates a metal (or free-electron-like plasma) from vacuum, the electromagnetic surface modes are often called *surface plasmaritons* (SPMs), a name we shall use below, not least because this name fits our treatment of the electron dynamics in the framework of the *jellium* (solid-state plasma) approach.

Although basic properties of electromagnetic surface waves have been studied since the turn of the 19th century, starting with the theoretical works of Zenneck [1], Sommerfeld [2,3], and Hörschelmann [4,5], the interest and the number of studies of surface polaritons increased significantly by the initial works of Otto [6], Kretschmann [7], and Raether [8–10]. These authors pointed out how surface polaritons could be generated (approximately) using attenuated or frustrated total reflection methods.

To a large extent, much of the basic understanding of the macroscopic and semiclassical (field-unquantized) properties of surface polaritons (and plasmaritons) were in place in the beginning of the 1980s. Good general accounts of the basic theory and its many diverse applications can be found in Refs. [11–13]. More recently, studies aimed at technological applications of SPMs (so-called plasmonics) have attracted much attention [14–17] and, in recent years, research on the border of quantum optics and plasmonics has emerged as a rapidly growing field of study entitled quantum plasmonics [18–21].

SPMs (and in a broader context polaritons) are *eigenmodes* of electromagnetic fields bound to a surface, and as such these modes are unobservable. All observations require an externally impressed excitation method, and the SPM appears as a resonance in all methods; cf. the methods of Sommerfeld (a dipole over a conducting surface), Otto, Kretschmann, Raether, and others.

Sharp-boundary models have a prominent position in the theory of SPMs and, in the long-wavelength regime, where spatial nonlocality (spatial dispersion) often can be neglected, a survey of the literature reveals that textbook boundary conditions, with neglect of possible surface charges, are used universally. This means that the boundary is electromagnetically passive, and the derived eigenmode dispersion relation becomes particularly simple; see Sec. II. If spatial dispersion effects, which are important at short wavelengths, are included, additional boundary conditions (ABCs) must be included even in the framework of sharp-boundary plasmariton models [11,22]. The various ABCs suggested over the

*okeller@physics.aau.dk

years, in one way or another, give rise to surface charges and currents. Even in the absence of spatial dispersion, the inevitably present electron density variations (in the surface region) give rise to microscopic surface currents [23]. Here we call a surface carrying charge or current an electrodynamically active surface (or boundary). In the wake of our recently developed wave mechanical and second-quantized theories for bulk and surface plasmons [24] and for bulk plasmaritons [25], we establish in this paper covariant wave-mechanical and second-quantized descriptions of SPMs. To a certain extent, our covariant formalism was inspired by a theory for covariant photon wave mechanics of evanescent fields [26], an alternative to the pioneering Carniglia and Mandel triplet-photon description of such fields [27].

The paper is organized as follows. In Sec. II, we discuss the shortcomings of the spatially local classical standard theory for SPMs [11–13,28]. The dispersion relation of the eigenmodes usually is obtained using the textbook boundary conditions at the surface [29]. For a SPM with active boundary electrodynamics, these conditions are insufficient because a dynamic component of the electron current density incorrectly is omitted, a component necessary for upholding charge conservation [30,31]. The surface current density sheet model has its roots in an electric-dipole approximation to the selvedge dynamics (discussion in Sec VI). Section II is closed with a general expression for the SPM dispersion relation with an active boundary, yet with the elimination of the surface current density in favor of the prevailing field left to the analysis in Sec. VI.

In Sec. III, the covariant theory of evanescent plamariton fields is presented. In the covariant formalism, four kinds of photons appear: Two transverse photons (T_1, T_2), a longitudinal photon (L), and a scalar photon (S). The four photons are related to the covariant four-potential [32] subject to the Lorenz-gauge constraint [33]. Although the covariant theory is a standard formalism in relativistic quantum electrodynamics [34–36], it has turned out to be of substantial importance in nonrelativistic near-field electrodynamics [38], not least in relation to studies of evanescent fields [37,38].

In Sec. IV, the covariant photon-wave mechanical theory of SPMs in the wave vector-time domain is established, paying particular attention to the four-potential state tied to a propagating electron sheet mode. In Sec. V, the covariant second-quantized description of SPMs is given. This formalism is based on the Heisenberg equations for the contravariant four-potential annihilation operators.

In Sec. VI, a self-consistent integral equation for the local electromagnetic field in the selvedge is derived, and from this a constitutive relation between the surface current density and the electric field in vacuum just outside the current sheet is established. On the basis of the constitutive relation, the final expression for the SPM dispersion relation with active boundary conditions is derived. The small extension of the selvedge makes it possible to neglect the field retardation across the selvedge profile, and as a consequence obtain a somewhat simpler form of the dispersion relation—in fact, a form analogous to that of the passive boundary case, just with an effective dielectric function showing spatial dispersion stemming from the selvedge. It is beyond the scope of the present paper to develop a microscopic formalism treating the selvedge response beyond the electric-dipole approximation. Some remarks on the covariant theory in a broader framework are given in Sec. X.

A quantitative microscopic study of the SPM dispersion relation with an electrodynamically active surface is presented in Sec. VII, where we model the selvedge as a quantum well (QW). This model can with the modest modification also be used to study SPMs on a metal surface covered with an conducting overlayer. From the one-electron microscopic conductivity tensor [taken in the low-temperature limit (approximation)], we derive a compact expression for the QW surface current density. To clarify the role of the QW current densities parallel and perpendicular to the jellium surface, we derive explicit theoretical results for the SPM dispersion in the diamagnetic and paramagnetic conductivity response limits. In the diamagnetic case, the dynamic surface electron motion is parallel to the surface and in the paramagnetic case the surface current density predominantly is perpendicular to the surface. Numerical results for the SPM dispersion relation are presented for one-level (diamagnetic response) and two-level (paramagnetic response) QWs.

In Sec VIII, the connection between the SPM and the quasiparticle bulk plasmariton is studied. Furthermore, the physics of the T photons tied to the surface plasmariton is discussed, and a comparison of similarities and differences of the covariant theory for T-photon tunneling [26,38] and the tied T-photon picture of the SPM is presented. The relation between spatial photon localization and the extension of the source region for the SPM's T photons is clarified.

In Sec. IX, remarks on SPM interaction with an external prescribed gauge field are given. An outlook is presented in Sec. X. In particular, we suggest that the SPM theory might be useful in Möbius band electrodynamics, cavity QED, and for investigations of accelerated solid-state plasmas. In Sec. X, we also compare key points in our trio (Refs. [24,25] and this paper) of papers on plasmon and plasmariton quantum physics. In Sec. XI, we present a summary including a schematic diagram showing the connections between the central fragments of the SPM theory developed in the present paper.

II. CRITICISM OF THE SPATIALLY LOCAL STANDARD THEORY FOR SURFACE PLASMARITONS

A. Dynamic boundary conditions

It may come as a surprise to the reader that we start our establishment of the quantum theory for SPMs with a discussion (correction) of the standard (textbook) boundary conditions for the electromagnetic field at a sharp boundary. However, we shall realize below that these—perhaps better-called jump (or in German saltus) conditions—play an important role.

Let us assume that the jellium occupies the $z > 0$ half space described in a Cartesian (x, y, z)-coordinate system, the rest of the space ($z < 0$) being vacuum. The jump in a given field component, with generic name F, across the $z = 0$-plane, we denote by

$$\|F\| \equiv F(0^+) - F(0^-). \tag{1}$$

Without loss of essential generality, let the real wave vector of a p-polarized monochromatic (ω) electromagnetic field along the surface surface plane ($\mathbf{q}_\parallel$) be pointing in the x direction ($\mathbf{q}_\parallel = q_\parallel \hat{\mathbf{x}}$; $\hat{\mathbf{x}}$ being a unit vector in the positive x direction). The (macroscopic) electric ($\mathbf{E}$) and magnetic ($\mathbf{B}$) fields hence have the form

$$\mathbf{E}(x, z, t) = \begin{pmatrix} E_x(z; q_\parallel, \omega) \\ 0 \\ E_z(z; q_\parallel, \omega) \end{pmatrix} e^{i(q_\parallel x - \omega t)}, \tag{2}$$

$$\mathbf{B}(x, z, t) = \begin{pmatrix} 0 \\ B_y(z; q_\parallel, \omega) \\ 0 \end{pmatrix} e^{i(q_\parallel x - \omega t)}, \tag{3}$$

with amplitudes in the mixed (z)-$(q_\parallel, \omega)$ domain. The textbook field jump conditions (also used in the most research literature) are [29]

$$\|E_x\| = 0 \text{ (i)}, \quad \|B_y\| = -\mu_0 J_x^S \text{ (ii)}, \quad \|D_z\| = \rho^S \text{ (iii)}, \tag{4}$$

where $J_x^S \equiv J_x^S(0; q_\parallel, \omega)$ is the x component of the surface (superscript S) current density and $\rho^S \equiv \rho^S(0; q_\parallel, \omega)$ is the surface charge density. (ii) and (iii) follow from the Maxwell's equations, and thus hold in general, but (i) is *correct only if the surface current density, $\mathbf{J}^S(0; q_\parallel, \omega)$, has no component perpendicular to the plane of the surface* [$J_z^S(0; q_\parallel, \omega) = 0$]. The generally wrong condition $J_z^S(0; q_\parallel, \omega) = 0$ originates in a *brute force* extension of the zero-frequency condition $J_z^S(0; q_\parallel, \omega = 0)$ to finite frequencies. At $\omega = 0$, the current density can of course not posses any z component, but for $\omega \neq 0$ nothing prevents an oscillatory component from existing perpendicular to the surface plane. The reader should here remember that an ideal infinitely thin surface layer physically is a mathematical truncation of a layer of finite thickness (see Secs. VI A and VI B). In layers so thin that QW phenomena play a role, the situation with $J_z^S(0; q_\parallel, \omega) \neq 0$ is well-known [39]. The neglect of the J_z^S-component also has the fatal consequence that the equation of continuity for the charge *is not* satisfied in general.

The general *dynamic* ($\omega \neq 0$) jump conditions have been derived previously [30,31,40] and can be expressed explicitly as follows for p-polarized fields:

$$\|E_x\| = \frac{1}{\varepsilon_0} \frac{q_\parallel}{\omega} J_z^S, \tag{5}$$

$$\|D_z\| = \frac{q_\parallel}{\omega} J_x^S, \tag{6}$$

$$\|B_y\| = -\mu_0 J_x^S, \tag{7}$$

noting that the equation of continuity has been used to eliminate ρ^S in favor of J_x^S in Eq. (6).

We name the boundary conditions *passive* if one can use the approximation $\mathbf{J}^S(0; q_\parallel, \omega) = \mathbf{0}$. If either $J_x^S(0; q_\parallel, \omega)$ or $J_z^S(0; q_\parallel, \omega)$ (or both) are nonvanishing, we speak of *active* boundary conditions (or just an active surface). As we shall realize below, a SPM eigenmode *always* has active jump conditions and a quantum theory can only be established in a rigorous sense under active saltus conditions (see Secs. IV and V).

To determine the dispersion relation for SPMs, two of the three jump conditions in Eqs. (5)–(7) have to be used. Since it follows from the Maxwell's equation, $\nabla \times \mathbf{B} = \mu_0 \mathbf{J} - i\mu_0 \omega \mathbf{D}$ [$\mathbf{D} = \varepsilon_0 \varepsilon(\omega) \mathbf{E}$ in the long-wavelength limit $\varepsilon(q \to 0, \omega) \equiv \varepsilon(\omega)$] that

$$\|B_y\| = -\mu_0 \frac{\omega}{q_\parallel} \|D_z\|, \tag{8}$$

a result which also follows directly from Eqs. (6) and (7), the dispersion relation is obtained using Eq. (5) together with either Eq. (6) or Eq. (7).

The standard theory for spatially local SPMs is based on the use of passive boundary conditions, so one can pick two of the three $\|E_x\| = \|B_y\| = \|D_z\| = 0$, as wished. For a lossless jellium with $\varepsilon(\omega) = 1 - (\omega_p/\omega)^2$, the dispersion relation becomes (as is well-known [11,13])

$$q_\parallel = \frac{\omega}{c} \left[\frac{\varepsilon(\omega)}{1 + \varepsilon(\omega)} \right]^{1/2} = \frac{\omega}{c} \left[\frac{\omega^2 - \omega_p^2}{2\omega^2 - \omega_p^2} \right]^{1/2}. \tag{9}$$

The dispersion relation has two branches: (i) The Brewster branch, existing only for $\omega \geqslant \omega_p$ [$0 \leqslant \varepsilon(\omega) < 1$], and radiative in vacuum, and (ii) the Fano branch describing bound (tied) surface modes, with $1 + \varepsilon(\omega) = 2 - (\omega_p/\omega)^2 < 0$. The bound Fano modes all have frequencies below the long-wavelength ($q \to 0$) surface plasma frequency, $\omega_p^S = \omega_p/\sqrt{2}$.

B. Surface plasmaritons with active surface

The eigenmodes can be obtained from the ansatz (vacuum, V; jellium, J),

$$E_x^V(z; q_\parallel, \omega) = A_V e^{-iq_\perp^0 z}, \quad E_z^V(z; q_\parallel, \omega) = \frac{q_\parallel}{q_\perp^0} A_V e^{-iq_\perp^0 z}, \tag{10}$$

$$E_x^J(z; q_\parallel, \omega) = A_J e^{iq_\perp z}, \quad E_z^J(z; q_\parallel, \omega) = -\frac{q_\parallel}{q_\perp} A_J e^{iq_\perp z}, \tag{11}$$

where

$$q_\perp^0 = \left[\left(\frac{\omega}{c} \right)^2 - q_\parallel^2 \right]^{1/2}, \tag{12}$$

$$q_\perp = \left[\left(\frac{\omega}{c} \right)^2 \varepsilon(\omega) - q_\parallel^2 \right]^{1/2}. \tag{13}$$

The p-polarized ansatz given above is guaranteed divergence-free ($\nabla \cdot \mathbf{E} = 0$) in both the vacuum and jellium domains. From the dynamic jump conditions in Eqs. (5) and (6), one obtains

$$A_J - A_V = \frac{1}{\varepsilon_0} \frac{q_\parallel}{\omega} J_z^S, \tag{14}$$

$$\frac{\varepsilon(\omega)}{q_\perp} A_J + \frac{1}{q_\perp^0} A_V = -\frac{1}{\varepsilon_0 \omega} J_x^S, \tag{15}$$

and hence in the surface active case, the following eigenmode condition for the SPMs:

$$\frac{1}{q_\parallel} (A_V - A_J) J_x^S = \left(\frac{\varepsilon(\omega)}{q_\perp} A_J + \frac{1}{q_\perp^0} A_V \right) J_z^S. \tag{16}$$

Returning to Eqs. (14) and (15), it is possible to eliminate J_x^S and J_z^S in favor of the prevailing field in the selvedge as we shall realize in Secs. VI A and VI B. In turn, one can use the resulting equations to derive the eigenmode condition (dispersion relation) in the presence of an active surface; see Sec. VI C.

In the passive surface case ($\mathbf{J}^S = \mathbf{0}$), Eqs. (14) and (15) give the determinant ($|\ldots|$) eigenmode condition,

$$\begin{vmatrix} 1 & -1 \\ \frac{\varepsilon(\omega)}{q_\perp} & \frac{1}{q_\perp^0} \end{vmatrix} = 0 \Leftrightarrow q_\perp + q_\perp^0 \varepsilon(\omega) = 0, \tag{17}$$

leading to the dispersion relation cited in Eq. (9), as is well-known.

III. COVARIANT DESCRIPTION OF EVANESCENT PLASMARITON FIELD

A. Near-field electrodynamics in the Lorenz gauge

In nonrelativistic quantum electrodynamics, one most often uses the Coulomb gauge for the quantization procedure because this choice simplifies the theoretical formalism, in general [32]. Although the Coulomb gauge also can be used in relativistic QED, it has the disadvantage that it is not *manifest* covariant. For most detailed relativistic calculations, it is of importance to keep track of manifest covariance. From this point of view, it is preferable to use the Lorenz gauge (or some other relativistically covariant gauge). In the Lorenz gauge, the vector ($\mathbf{A}$) and the scalar (Φ) potentials are treated symmetrically, with the result that four types of photons enter the quantization procedure: (i) Two transversely polarized ($T1$ and $T2$ photons), (ii) one longitudinal polarized (L photon), and (iii) one scalar photon (S photon).

However, it was pointed out by one of the present authors (Keller) more than a decade ago that the covariant Lorenz gauge formalism may be preferable also in nonrelativistic QED in connection to studies in *near-field quantum electrodynamics* [37]. Here, it is furthermore sometimes convenient to transform the L- and S-photon set, to a new set consisting of a gauge photon (G photon) and a so-called near-field photon (NF photon) [37]. The G photon can be eliminated from the formalism by a transformation *within* the Lorenz gauge.

Evanescent electromagnetic fields fall within the definition of what a near field is [38]. The manifest evanescent Lorenz gauge description was shown in 2012 to provide a physically transparent description of the photon tunneling effect [26], and in the book *Light—The Physics of the Photon* [38], many details of this tunneling effect are discussed. In the following, we shall take advantage of the knowledge obtained from the photon tunneling effect in our quantum physical theory for SPMs. Since a number of calculations in this section run parallel to those for the tunneling phenomenon, we will often refer the reader to the above-mentioned book for calculational details.

B. Lorenz gauge and the four-potential in the rim (near-field) zone of a sheet

Using four-vector notation, with the summation over repeated lower and upper indices kept implicit, the inhomogeneous wave equations for the components ($\mu = 0-3$) of the contravariant four-potential $\{A^\mu\} \equiv (A^0 = \Phi/c, \mathbf{A})$ read

$$\partial^\nu \partial_\nu A^\mu(x) = -\mu_0 J^\mu(x), \quad \mu = 0-3, \tag{18}$$

where $\{J^\mu(x)\} = (J^0 = c\rho, \mathbf{J})$ is the contravariant four-current density, and $\{\partial_\mu\} = (c^{-1}\partial/\partial t, \nabla)$ and $\{x^\mu\} = (ct, \mathbf{r})$, $x = (\mathbf{r}, ct)$. Metric signature $(-1, 1, 1, 1)$ is used here and in what follows. The complete solution to Eq. (18) can be written in the integral form

$$\{A^\mu(x)\} = \{A^\mu_{\text{inc}}(x)\} + \mu_0 \int_{-\infty}^{\infty} D_R(x-x')\{J^\mu(x')\} d^4x', \tag{19}$$

where $\{A^\mu_{\text{inc}}\}$ is the incident (inc) four-potential and with $X = x - x'$ and $\tau = t - t'$,

$$D_R(X) = \frac{1}{c} g(X) = \frac{1}{c} g(R, \tau) = \frac{1}{4\pi R}\delta\left(\frac{R}{c} - \tau\right) \tag{20}$$

is the retarded (R) scalar propagator [34,35,39].

For use in relation to SPMs, the components of *all* vector fields $\{\mathcal{F}^\mu(\mathbf{r}, t)\}$ have the generic form

$$\mathcal{F}^\mu(\mathbf{r}, t) = \mathcal{F}^\mu(z; q_\parallel, \omega) e^{i(q_\parallel x - \omega t)}, \tag{21}$$

cf. Eqs. (2) and (3). Leaving out the reference to $q_\parallel$ and ω, that is,

$$\mathcal{F}^\mu(z; q_\parallel, \omega) \equiv \mathcal{F}^\mu(z), \tag{22}$$

one obtains

$$A^\mu(z) = A^\mu_{\text{inc}}(z) + \mu_0 \int_{-\infty}^{\infty} g(Z) J^\mu(z') dz', \tag{23}$$

where $Z = z - z'$ and

$$g(Z) = \frac{i}{2q_\perp^0} e^{iq_\perp^0 |Z|}. \tag{24}$$

When $q_\parallel > q_0 \equiv \omega/c$, $q_\perp^0$ [Eq. (12)] becomes purely imaginary, i.e., $q_\perp^0 = i\kappa_\perp^0$, with

$$\kappa_\perp^0 = \left[q_\parallel^2 - \left(\frac{\omega}{c}\right)^2\right]^{1/2} \quad (>0). \tag{25}$$

The four-potential related to the evanescent modes in vacuum thus has the form

$$\sim e^{-\kappa_\perp^0 |Z|} \exp\left[i(q_\parallel x - \omega t)\right] \tag{26}$$

in the two domains $Z \lessgtr 0$.

C. Evanescent *T*, *L*, and *S* potentials of a surface plasmariton

Let us denote the z-dependent surface current density by

$$\mathbf{J}^S(z) = \mathbf{I}\delta(z). \tag{27}$$

As shown and analyzed in detail in Ref. [38], in connection to photon tunneling, the T, L, and S parts of the four-potential from a p-polarized sheet current density placed in otherwise vacuum is given by

$$\mathbf{A}_T(z) = \frac{e^{\kappa_\perp^0 z}}{2\varepsilon_0 \kappa_\perp^0 \omega^2} (\hat{\mathbf{y}} \times \mathbf{q}_<)(\hat{\mathbf{y}} \times \mathbf{q}_<) \cdot \mathbf{I}, \quad z < 0, \tag{28}$$

$$\mathbf{A}_L(z) = \frac{e^{\kappa_\perp^0 z}}{2\varepsilon_0 \kappa_\perp^0 \omega^2} \mathbf{q}_< \mathbf{q}_< \cdot \mathbf{I}, \quad z < 0, \tag{29}$$

$$A_S(z) = \frac{e^{\kappa_\perp^0 z}}{2\varepsilon_0 \kappa_\perp^0 c\omega} \mathbf{q}_< \cdot \mathbf{I}, \quad z < 0, \tag{30}$$

where

$$\mathbf{q}_< = q_\parallel \hat{\mathbf{x}} - i\kappa_\perp^0 \hat{\mathbf{z}}, \; z < 0. \tag{31}$$

In the homogeneous jellium, which occupies the half-space $z > 0$, the expressions for the various parts of the potentials are obtained from Eqs. (28)–(30), making the replacements $z \to -z$,

$$\kappa_\perp^0 \Rightarrow \kappa_\perp = \left[q_\parallel^2 - \left(\frac{\omega}{c}\right)^2 \varepsilon(\omega)\right]^{1/2}, \tag{32}$$

and $\mathbf{q}_< \Rightarrow \mathbf{q}_>$, where

$$\mathbf{q}_> = q_\parallel \hat{\mathbf{x}} + i\kappa_\perp \hat{\mathbf{z}}, \; z > 0. \tag{33}$$

Hence,

$$\mathbf{A}_T(z) = \frac{e^{-\kappa_\perp z}}{2\varepsilon_0 \kappa_\perp \omega^2} (\hat{\mathbf{y}} \times \mathbf{q}_>)(\hat{\mathbf{y}} \times \mathbf{q}_>) \cdot \mathbf{I}, \quad z > 0, \tag{34}$$

$$\mathbf{A}_L(z) = \frac{-e^{\kappa_\perp z}}{2\varepsilon_0 \kappa_\perp \omega^2} \mathbf{q}_> \mathbf{q}_> \cdot \mathbf{I}, \quad z > 0, \tag{35}$$

$$A_S(z) = \frac{e^{-\kappa_\perp z}}{2\varepsilon_0 \kappa_\perp c\omega} \mathbf{q}_> \cdot \mathbf{I}, \quad z > 0. \tag{36}$$

The expressions for associated electric fields follow from

$$\mathbf{E}_T(z) = i\omega \mathbf{A}_T(z), \quad z \lessgtr 0, \tag{37}$$

$$\mathbf{E}_L(z) = i\omega \mathbf{A}_L(z) - ic\mathbf{q}_\lessgtr A_S(z). \quad z \lessgtr 0. \tag{38}$$

At this point, one should recall that the Coulomb interaction between stationary pairs of charged particles (∼ electrons) in the covariant Lorenz gauge is described as an exchange of scalar photons [32,38]. If the two particles move relatively to each other, the longitudinal photon also enters as a part of the interaction [38].

IV. PHOTON-WAVE MECHANICAL THEORY OF SURFACE PLASMARITONS

A. Four-potential in the wave vector (Q)-time domain

Since photon-wave mechanics is known to take a particularly simple form in the wave-vector-time domain [38], let us transform the expressions for $\mathbf{A}_T(Z)$, $\mathbf{A}_L(z)$, and $A_S(z)$ to the 1D Fourier space. For later convenience, we also make the notational replacement $q_\parallel \to Q_\parallel$. The components of the monochromatic (ω) four-potential, $\{A^\mu(\mathbf{r}, t)\}$, with wave vector $\mathbf{Q}_\parallel = Q_\parallel \hat{\mathbf{x}}$ along the surface thus has the integral form

$$A^\mu(\mathbf{r}, t) = \left[(2\pi)^{-1} \int_{-\infty}^{\infty} A^\mu(Q_\perp) e^{iQ_\perp z} dQ_\perp\right] e^{i(Q_\parallel x - \omega t)}, \tag{39}$$

where

$$A^\mu(Q_\perp) = \int_{-\infty}^{\infty} A^\mu(z) e^{-iQ_\perp z} dz \tag{40}$$

is the Fourier integral transform of $A^\mu(z)$.

From a calculational point of view, it is useful first to determine the Fourier transform of the scalar potential. From Eqs. (30) and (36), it appears that

$$A_S(Q_\perp) = \frac{1}{2\varepsilon_0 c\omega}\left[\mathbf{q}_< \cdot \mathbf{I} \int_{-\infty}^{0} \frac{1}{\kappa_\perp^0} e^{(\kappa_\perp^0 - iQ_\perp)z} dz \right.$$

$$\left. + \mathbf{q}_> \cdot \mathbf{I} \int_0^\infty \frac{1}{\kappa_\perp} e^{-(\kappa_\perp + iQ_\perp)z} dz\right], \tag{41}$$

and hence

$$A_S(Q_\perp) = \frac{1}{2\varepsilon_0 c\omega}\left[\frac{\mathbf{q}_<}{\kappa_\perp^0(\kappa_\perp^0 - iQ_\perp)} + \frac{\mathbf{q}_>}{\kappa_\perp(\kappa_\perp + iQ_\perp)}\right] \cdot \mathbf{I}. \tag{42}$$

The result in Eq. (42) is reduced to

$$A_S(Q_\perp) = \frac{1}{\varepsilon_0 c\omega} \frac{\mathbf{Q} \cdot \mathbf{I}}{(\kappa_\perp^0)^2 + Q_\perp^2} = \frac{1}{\varepsilon_0 c\omega} \frac{\mathbf{Q} \cdot \mathbf{I}}{Q^2 - q_0^2}, \tag{43}$$

where

$$\mathbf{Q} = Q_\parallel \hat{\mathbf{x}} + Q_\perp \hat{\mathbf{z}} \tag{44}$$

if there is vacuum to both sides (half spaces) of the current density sheet ($\kappa_\perp \Rightarrow \kappa_\perp^0$). The expression in Eq. (43) has been used to study the optical (photon) tunneling between two current density sheets previously [38].

The Lorenz gauge condition

$$\mathbf{A}_L = \frac{q_0}{q^2} \mathbf{q} A_S, \tag{45}$$

with $\mathbf{q} = \mathbf{q}_<$ ($\mathbf{q}_>$) in the half space $z < 0$ ($z > 0$), immediately gives for the longitudinal mode

$$\mathbf{A}_L(Q_\perp) = \frac{\mu_0}{2}\left[\frac{1}{\kappa_\perp^0(\kappa_\perp^0 - iQ_\perp)} \frac{\mathbf{q}_<\mathbf{q}_<}{q_<^2} + \frac{1}{\kappa_\perp(\kappa_\perp + iQ_\perp)} \frac{\mathbf{q}_>\mathbf{q}_>}{q_>^2}\right] \cdot \mathbf{I}. \tag{46}$$

A comparison of Eqs. (28) and (29) [Eqs. (34) and (35)] leads, with

$$\tilde{\mathbf{q}}_\lessgtr = \hat{\mathbf{y}} \times \mathbf{q}_\lessgtr, \tag{47}$$

immediately to the following result for the transverse potential:

$$\mathbf{A}_T(Q_\perp) = \frac{\mu_0}{2}\left[\frac{1}{\kappa_\perp^0(\kappa_\perp^0 - iQ_\perp)} \frac{\tilde{\mathbf{q}}_<\tilde{\mathbf{q}}_<}{q_<^2} + \frac{1}{\kappa_\perp(\kappa_\perp + iQ_\perp)} \frac{\tilde{\mathbf{q}}_>\tilde{\mathbf{q}}_>}{q_>^2}\right] \cdot \mathbf{I}. \tag{48}$$

B. Sheet surface current density

The surface current density used in Sec. II is given as

$$\mathbf{J}^S = \int_{-\infty}^{\infty} \mathbf{I}\delta(z) dz = \mathbf{I}, \tag{49}$$

and the surface charge density divided by c, $J^{0,S}$, is readily obtained via the equation of continuity. Thus,

$$J^{0,S} = \frac{1}{q_0} \mathbf{Q} \cdot \mathbf{I}. \tag{50}$$

The monochromatic contravariant sheet four-current density consequently is given by ($\mathbf{e_Q} = \mathbf{Q}/Q$)

$$\{J^\mu(\mathbf{Q}; t)\} = \left(\frac{Q}{q_0} \mathbf{e_Q} \cdot \mathbf{I}, \mathbf{I}\right) e^{-i\omega t} \tag{51}$$

in the wave-vector ($\mathbf{Q}$)-time domain.

C. Surface plasmariton: Four-potential state tied to propagating electron mode

Physical insight in the wave-mechanical theory of SPMs can be obtained by addressing the similarities and differences to the first-quantized theories of transverse, longitudinal, and scalar photons.

For this purpose, let us begin with the introduction of the following abbreviations:

$$\mathbf{S}_A(Q_\perp, Q_\parallel, \omega) = \frac{1}{2\varepsilon_0\omega}\left[\frac{\mathbf{q}_<}{\kappa_\perp^0(\kappa_\perp^0 - iQ_\perp)} + \frac{\mathbf{q}_>}{\kappa_\perp(\kappa_\perp + iQ_\perp)}\right], \tag{52}$$

$$\mathbf{L}_A(Q_\perp, Q_\parallel, \omega) = \frac{\mu_0}{2}\left[\frac{1}{\kappa_\perp^0(\kappa_\perp^0 - iQ_\perp)}\frac{\mathbf{q}_<\mathbf{q}_<}{q_<^2} + \frac{1}{\kappa_\perp(\kappa_\perp + iQ_\perp)}\frac{\mathbf{q}_>\mathbf{q}_>}{q_>^2}\right], \tag{53}$$

$$\mathbf{T}_A(Q_\perp, Q_\parallel, \omega) = \frac{\mu_0}{2}\left[\frac{1}{\kappa_\perp^0(\kappa_\perp^0 - iQ_\perp)}\frac{\tilde{\mathbf{q}}_<\tilde{\mathbf{q}}_<}{q_<^2} + \frac{1}{\kappa_\perp(\kappa_\perp + iQ_\perp)}\frac{\tilde{\mathbf{q}}_>\tilde{\mathbf{q}}_>}{q_>^2}\right]. \tag{54}$$

Note that

$$\mathbf{T}_A(Q_\perp, Q_\parallel, \omega) = \mathbf{L}_A(Q_\perp, Q_\parallel, \omega; \mathbf{q}_\lessgtr \Rightarrow \tilde{\mathbf{q}}_\lessgtr). \tag{55}$$

With the abbreviations in Eqs. (52)–(54), it appears from Eqs. (42), (46), and (48) that the monochromatic (ω) plane wave ($\mathbf{Q} = Q_\parallel\hat{\mathbf{x}} + Q_\perp\hat{\mathbf{z}}$) potentials are given by

$$A_S(\mathbf{Q}, t) = \mathbf{S}_A(Q_\perp, Q_\parallel, \omega)\cdot\mathbf{I}e^{-i\omega t}, \tag{56}$$

$$\mathbf{A}_L(\mathbf{Q}, t) = \mathbf{L}_A(Q_\perp, Q_\parallel, \omega)\cdot\mathbf{I}e^{-i\omega t}, \tag{57}$$

$$\mathbf{A}_T(\mathbf{Q}, t) = \mathbf{T}_A(Q_\perp, Q_\parallel, \omega)\cdot\mathbf{I}e^{-i\omega t}, \tag{58}$$

in the wave vector ($\mathbf{Q}$)-time domain. From Eq. (57), one may obtain an expression for the amplitude $A_L(\mathbf{Q}; t) = \mathbf{e_Q}\cdot\mathbf{A}_L(\mathbf{Q}; t)$, viz.,

$$A_L(\mathbf{Q}; t) = [\mathbf{L}_A(Q_\perp, Q_\parallel, \omega)\cdot\mathbf{e_Q}]\cdot\mathbf{I}e^{-i\omega t}, \tag{59}$$

utilizing that $\mathbf{L}_A$ is a symmetric tensor.

Since, for a generic $\mathcal{T}(Q_\perp, Q_\parallel, \omega)$,

$$\left(cQ - i\frac{\partial}{\partial t}\right)\mathcal{T}(Q_\perp, Q_\parallel, \omega)e^{-i\omega t} = (cQ - \omega)\mathcal{T}(Q_\perp, Q_\parallel, \omega)e^{-i\omega t}, \tag{60}$$

one can obtain the dynamical differential forms

$$\left(cQ - i\frac{\partial}{\partial t}\right)A_S(\mathbf{Q}; t) = (cQ - \omega)\mathbf{S}_A(Q_\perp, Q_\parallel, \omega)\cdot\mathbf{I}e^{-i\omega t}, \tag{61}$$

$$\left(cQ - i\frac{\partial}{\partial t}\right)A_L(\mathbf{Q}; t) = (cQ - \omega)[\mathbf{L}_A(Q_\perp, Q_\parallel, \omega)\cdot\mathbf{e_Q}]\cdot\mathbf{I}e^{-i\omega t}, \tag{62}$$

$$\left(cQ - i\frac{\partial}{\partial t}\right)\mathbf{A}_T(\mathbf{Q}; t) = (cQ - \omega)\mathbf{T}_A(Q_\perp, Q_\parallel, \omega)\cdot\mathbf{I}e^{-i\omega t} \tag{63}$$

for the SPM potentials. The dynamical equations above are form-identical to those for S, L, and T photons (two polarization types) driven by a certain current density [37]. In the photon case, we can think of free propagation of these modes (the right-hand-side of the equations equal to zero), although one physically has no net effect of the S and L photons ($A_S - A_L = 0$).

For SPMs (with active boundary conditions), the effective current densities appearing on the right-hand side of Eqs. (61)–(63) *always* are nonvanishing. Due to the fact that the same surface current density $\mathbf{I}$ (see Sec. VI B) enters all three dynamical equations, the SPM possesses an internal structure consisting of three (four) tied photons [$T(T1, T2)$, L, S] when the SPM is considered as a quasiparticle. In Sec. VIII, we discuss the SPM quasiparticle picture in some detail.

V. SECOND-QUANTIZED THEORY OF SURFACE PLASMARITONS

In Sec. III, a covariant potential description of evanescent surface fields originating in a sheet current density source was established, and in Sec. IV a related *classical* (first-quantized) photon-wave mechanical theory of SPMs was formulated. Limiting the analysis to monochromatic transverse, longitudinal, and scalar photons the coupled dynamical equations for these photon types were set up [Eqs. (61)–(63)]. In the following, we shall indicate how the photon-wave mechanical formulation of SPMs, when extended to the second-quantized level, constitutes a sector of covariant quantum electrodynamics (QED).

Let us denote the contravariant four-potential field annihilation operator for the mode $\mathbf{Q}$ by $\{\hat{a}^\mu(\mathbf{Q})\}$. In the Heisenberg picture, each of the four ($\mu = 0 - 3$) annihilation operators satisfies the Heisenberg equation

$$i\hbar\frac{\partial}{\partial t}\hat{a}^\mu(\mathbf{Q}; t) = [\hat{a}^\mu(\mathbf{Q}; t), \hat{H}_R] + [\hat{a}^\mu(\mathbf{Q}; t), \hat{H}_I], \tag{64}$$

where $\hat{H}_R$ and $\hat{H}_I$ are the radiation (R) and interaction (I) Hamilton operators, respectively [38]. From the Heisenberg equation above, one may obtain the following dynamical equation for $\{\hat{a}^\mu\}$:

$$\left(\frac{\partial}{\partial t} + icQ\right)\{\hat{a}^\mu(\mathbf{Q}; t)\} = \frac{i}{(2\varepsilon_0\hbar cQ)^{1/2}}\{\hat{J}^\mu(\mathbf{Q}; t)\}, \tag{65}$$

where

$$\{\hat{J}^\mu(\mathbf{Q}; t)\} = \int_{-\infty}^{\infty}\{\hat{J}^\mu(\mathbf{r}, t)\}e^{-i\mathbf{Q}\cdot\mathbf{r}}d^3r \tag{66}$$

is the spatial Fourier transform of the four-current density operator in direct space.

The second-quantized theory of SPMs with active boundary conditions constitutes a particular sector of the general QED theory—the Heisenberg equation for the four-potential field operator is given by Eq. (65). To establish the connection between the fundamental QED theory and the extension of the photon-wave mechanical theory of SPMs (Sec. IV) to the second-quantized level, rather than using a fixed Cartesian basis for $\{\hat{a}^\mu\}$, one projects $\{\hat{a}^\mu\}$ on the two (orthogonal) transverse unit vectors perpendicular to $\mathbf{Q}$, and one unit vector $\mathbf{Q}/Q$ along $\mathbf{Q}$. This leads to dynamical equations for $\hat{a}_S(\mathbf{Q};t)$, $\hat{a}_L(\mathbf{Q};t)$ and two transverse annihilation operators $\hat{a}_{T,s}(\mathbf{Q};t)$, $s = 1, 2$, belonging, e.g., to the photon helicity basis.

The manner in which the covariant quantized theory for the SPM may be connected to the general QED formalism runs in parallel for the S, L, $T1$, and $T2$ potential modes, so in the following it is sufficient to consider in detail the connection for the S mode, say.

It is known that the scaling

$$A_S(\mathbf{Q},\omega) = \left(\frac{\hbar}{2\varepsilon_0 cQ}\right)^{1/2} \alpha_S(\mathbf{Q},\omega) \tag{67}$$

leads to the second-quantized operator formalism for the scalar potential by extending the classical normal variable $\alpha_S(\mathbf{Q};\omega)$ to the operator level, i.e.,

$$\alpha_S(\mathbf{Q},\omega) \Rightarrow \hat{a}_S(\mathbf{Q};\omega). \tag{68}$$

The reader may find a comprehensive discussion of the formalism which leads to the extension cited in Eq. (68) in Chap. V of Ref. [32]. In particular, the covariant Heisenberg equation for the field operator $\hat{a}^\mu$ is established in Sec. VA3 of Ref. [32] of the interacting Dirac (or Schödinger) and Maxwell fields, and the covariant commutation rules are obtained in Sec. V B of Ref. [32]. The application of the general formalism to evanescent fields driven by a sheet current density is described in Chap. 19 of Ref. [38].

It appears from Eq. (56) that

$$\alpha_S(\mathbf{Q},\omega) = \left(\frac{2\varepsilon_0 cQ}{\hbar}\right)^{1/2} \mathbf{S}_A(Q_\perp, Q_\parallel,\omega)\cdot \mathbf{I}(Q_\parallel,\omega) \tag{69}$$

and thus

$$\hat{a}_S(\mathbf{Q};\omega) = \left(\frac{2\varepsilon_0 cQ}{\hbar}\right)^{1/2} \mathbf{S}_A(Q_\perp, Q_\parallel,\omega)\cdot \hat{\mathbf{I}}(Q_\parallel,\omega), \tag{70}$$

where $\hat{\mathbf{I}}(Q_\parallel,\omega)$ is the extension of the surface current density $\mathbf{I}(Q_\parallel,\omega)$ [Eq. (49)] to the operator level. The source vector, $\hat{\mathbf{I}}(Q_\parallel,\omega)$, in an operator in particle space. An explicit expression for $\hat{\mathbf{I}}(Q_\parallel,\omega)$ is not needed here. By a multiplication of Eq. (70) by $(cQ-\omega)\exp(-i\omega t)$, followed by an integration over all frequencies, one obtains

$$\begin{aligned}\int_{-\infty}^{\infty} (cQ-\omega)\hat{a}_S(\mathbf{Q},\omega)e^{-i\omega t}d\omega \\ = \left(\frac{2\varepsilon_0 cQ}{\hbar}\right)^{1/2} \int_{-\infty}^{\infty} (cQ-\omega)\mathbf{S}_A(Q_\perp, Q_\parallel,\omega)\cdot \hat{\mathbf{I}}(Q_\parallel,\omega) \\ \times e^{-i\omega t}d\omega.\end{aligned} \tag{71}$$

The Heisenberg equation for the mode annihilation operator for the scalar field therefore has the form

$$\begin{aligned}\left(\frac{\partial}{\partial t} + icQ\right)\hat{a}_s(\mathbf{Q};t) \\ = i\left(\frac{2\varepsilon_0 cQ}{\hbar}\right)^{1/2} \int_{-\infty}^{\infty} (cQ-\omega)\mathbf{S}_A(Q_\perp, Q_\parallel,\omega)\cdot \hat{\mathbf{I}}(Q_\parallel,\omega) \\ \times e^{-i\omega t}d\omega.\end{aligned} \tag{72}$$

A comparison of Eq. (72) and the general dynamical equation [Eq. (65)] shows that the time-dependent scalar current density mode operator is given by

$$\begin{aligned}\hat{\mathbf{J}}_S(\mathbf{Q};t) \\ = 2\varepsilon_0 cQ \int_{-\infty}^{\infty} (cQ-\omega)\mathbf{S}_A(Q_\perp, Q_\parallel,\omega)\cdot \hat{\mathbf{I}}(Q_\parallel,\omega)e^{-i\omega t}d\omega\end{aligned} \tag{73}$$

for a SPM with an active boundary. A self-consistent determination of $\hat{a}_S(\mathbf{Q};t)$ requires use of the field-dependent Schrodinger equation. In the framework of linear electrodynamics, the $\hat{\mathbf{I}}$ operator can be expressed in terms of the sheet current density and the field

$$\hat{\mathbf{E}} = i\omega(\hat{\mathbf{A}}_T + \hat{\mathbf{A}}_L) - ic\mathbf{q}_{\lessgtr}\hat{\mathbf{A}}_S \tag{74}$$

acting at the surface; see Secs. VI A and VI B. A discussion of the classical local field in the selvedge and the related surface current density is presented in Sec. VI.

The Heisenberg equation for the longitudinal mode annihilation operator, $\hat{a}_L(\mathbf{Q};t)$, can be obtained from Eq. (72), making the replacement $\mathbf{S}_A \Rightarrow \mathbf{L}_A\cdot\mathbf{e_Q}$, as obvious from Eqs. (56) and (59). The dynamical equations for the two transverse annihilation operators, $\hat{a}_{T,s}(\mathbf{Q};t)$, $s = 1, 2$ follow by use of, for instance, the helicity basis projections of $\mathbf{A}_T(\mathbf{Q};\mathbf{t})$, namely,

$$\begin{aligned}(\mathbf{U} - \mathbf{e_Q e_Q})\cdot \mathbf{A}_T(\mathbf{Q};t) \\ = \mathbf{e}_+^*\mathbf{e}_+\cdot\mathbf{A}_T(\mathbf{Q};t) + \mathbf{e}_-^*\mathbf{e}_-\cdot\mathbf{A}_T(\mathbf{Q};t),\end{aligned} \tag{75}$$

where $\mathbf{e}_\pm(\mathbf{Q}/Q)$ are positive (+) and negative (−) helicity unit vectors belonging to a given $\mathbf{Q}$ direction [38]. The two replacements $\mathbf{S}_A \Rightarrow \mathbf{e}_\pm^*\mathbf{e}_\pm\cdot\mathbf{T}_A$ afterward are used on the right side of Eq. (72) to obtain the dynamical equations for $\hat{a}_{T,s}$, $s = 1, 2$.

VI. LOCAL FIELD IN THE SELVEDGE. SURFACE CURRENT DENSITY, $\mathbf{J}^S(0;q_\parallel,\omega)$

A. Fundamental selvedge electrodynamics

At the outermost atomic layers of the metal-semiconductor surface, here treated in the jellium approximation, the electron density changes from zero (in vacuum) to its homogeneous jellium bulk value. The basis for a determination of the ideal surface current density, $\mathbf{J}^S(0;q_\parallel,\omega) = J_x^S(0;q_\parallel,\omega)\hat{\mathbf{x}} + J_z^S(0;q_\parallel,\omega)\hat{\mathbf{z}}$, is a calculation of the local electric field, $\mathbf{E}(z;q_\parallel,\omega)$, inside the selvedge region, followed by a determination of the associated selvedge (superscript SE) current density, $\mathbf{J}^{\mathrm{SE}}(z;q_\parallel,\omega)$. Over the years, various authors have studied the selvedge problem using different approaches

[8,11,29,41]. For what follows, the electromagnetic propagator formalism [41] is particularly convenient. Once the current density across the selvedge has been determined, the surface current density, $\mathbf{J}^S(0; q_\parallel, \omega)$, is obtained considering the selvedge as a sort of electric-dipole (ED) absorber and radiator [40]. For notational simplicity, we leave out the reference to $q_\parallel$ and ω below; cf. Eq. (22).

In the absence of an external driving field, the local electric field inside the selvedge profile, $\mathbf{E}^{\rm SE}(z)$, is related to the selvedge current density, $\mathbf{J}^{\rm SE}(z)$, by an integral relation extending over the selvedge, viz.,

$$\mathbf{E}^{\rm SE}(z) = -i\mu_0\omega \int_{\rm SE} \mathbf{G}(z, z') \cdot \mathbf{J}^{\rm SE}(z')dz'. \tag{76}$$

Depending on one's aim, various field propagator $[\mathbf{G}(z, z')]$ choices can be made. In the selvedge region, the propagator has two parts: (i) a part, $\mathbf{G}_D$, related to the *direct* (D) propagation between the source (z') and observation (z) planes and (ii) an *indirect* (I) part, $\mathbf{G}_I$, reaching the plane of observation upon reflection from the bulk jellium [40]. If one uses the vacuum propagator, the direct part depends on the difference $z - z'$, only, i.e., $\mathbf{G}_D(z - z')$. Electronic screening effects may be incorporated in $\mathbf{G}_D$, giving the general form $\mathbf{G}_D(z, z')$. In the jellium bulk, it is often useful to use the so-called semiclassical infinite-barrier model, giving a nonlocal screened propagator which allows one to study the roles of bulk plasmons, bulk plasmaritons, and single-electron excitations in the jellium [40].

To close the eigenmode loop for the local selvedge field the selvedge current density must be related to the prevailing selvedge field. In the absence of nonlinear electrodynamic effects, these quantities are connected linearly and nonlocally (in space) as follows [40]:

$$\mathbf{J}^{\mathbf{SE}}(z) = \int_{\rm SE} \boldsymbol{\sigma}^{\rm SE}(z, z') \cdot \mathbf{E}^{\rm SE}(z')dz', \tag{77}$$

where

$$\boldsymbol{\sigma}^{\rm SE}(z, z') = \boldsymbol{\sigma}(z, z') - \boldsymbol{\sigma}^{\rm bulk}(z, z') \tag{78}$$

is the microscopic selvedge conductivity response tensor, given as the difference between the "exact" conductivity tensor, $\boldsymbol{\sigma}(z, z')$, and the bulk conductivity tensor. By combining Eqs. (76) and (77), one obtains a homogenous integral equation

$$\mathbf{E}^{\rm SE}(z) = \int_{\rm SE} \mathbf{K}(z, z') \cdot \mathbf{E}^{\rm SE}(z')dz' \tag{79}$$

for the local field *inside* the selvedge profile. The dyadic kernel, $\mathbf{K}(z, z')$, is given by

$$\mathbf{K}(z, z') = -i\mu_0\omega \int_{\rm SE} \mathbf{G}(z, z'') \cdot \boldsymbol{\sigma}^{\rm SE}(z'', z')dz''. \tag{80}$$

Due to the fact that the selvedge conductivity tensor has the following sum over tensor-product structure [39]:

$$\boldsymbol{\sigma}^{\rm SE}(z, z') = \sum_N A_N \mathbf{B}_N(z)\mathbf{C}_N(z') - \sum_n a_n \mathbf{b}_n(z)\mathbf{c}_n(z'), \tag{81}$$

it is possible to convert the integral problem [Eq. (79)] into a matrix problem for eigenmode determination [39,42]. In a forthcoming theoretical paper, dealing with current density functional formalism extending the standard density functional theory to the transverse high-frequency regime, Eq. (81) will be used.

In Eq. (81), N and n run over pairs of (many-body) energy eigenstates and $\mathbf{B}_N(z)$ $[\mathbf{C}_N(z')]$ and $\mathbf{b}_n(z)$ $[\mathbf{c}_n(z')]$ are transition current densities related to $\boldsymbol{\sigma}(z, z')$ and $\boldsymbol{\sigma}^{\rm bulk}(z, z')$, respectively. Note that these quantities are taken at z and z' planes.

B. Surface current density (I). Surface electric field on the vacuum side $[\mathbf{E}^V(0^-)]$

It appears from Eqs. (27), (49), and (77) that the integral of the z-dependent selvedge current density, $\mathbf{J}^{\rm SE}(z)$, is to be identified as the surface current density, $\mathbf{I}$, given by

$$\mathbf{I} = \int_{\rm SE} \mathbf{J}^{\rm SE}(z)dz = \int_{\rm SE} \boldsymbol{\sigma}^{\rm SE}(z, z') \cdot \mathbf{E}^{\rm SE}(z')dz'dz. \tag{82}$$

For consistency, the electric field used in Sec. II B on the vacuum side at $z = 0^-$, viz.,

$$\mathbf{E}^V(0^-) = A_V\left(\hat{\mathbf{x}} + \frac{q_\parallel}{q_\perp^0}\hat{\mathbf{z}}\right), \tag{83}$$

must be connected to the local selvedge field, $\mathbf{E}^{\rm SE}(z)$, by an integral relation of the following from

$$\mathbf{E}^V(0^-) \equiv \frac{\int_{\rm SE} \boldsymbol{\sigma}^{\rm SE}(z, z') \cdot \mathbf{E}^{\rm SE}(z')dz'dz}{\int_{\rm SE} \boldsymbol{\sigma}^{\rm SE}(z, z')dz'dz}. \tag{84}$$

Thus,

$$\mathbf{I} = \mathbf{S} \cdot \mathbf{E}^V(0^-), \tag{85}$$

where

$$\mathbf{S} = \int_{\rm SE} \boldsymbol{\sigma}^{\rm SE}(z, z')dz'dz. \tag{86}$$

C. Dispersion relation with active boundary conditions

To determine the dispersion relation from Eqs. (14) and (15), one writes the constitutive relation in Eq. (85) in the 2 x 2-matrix form

$$\begin{pmatrix} J_x^S \\ J_z^S \end{pmatrix} = \begin{pmatrix} S_{xx} & S_{xz} \\ S_{zx} & S_{zz} \end{pmatrix} \begin{pmatrix} 1 \\ \frac{q_\parallel}{q_\perp^0} \end{pmatrix} A_V. \tag{87}$$

By inserting the expressions for J_x^S and J_z^S into Eqs. (14) and (15), and setting the determinant of the two homogeneous equations for A_J and A_V to zero, one obtains from microscopic electrodynamics the following SPM dispersion relation in implicit form:

$$q_\perp + \varepsilon(\omega)q_\perp^0 + \frac{q_\perp^0}{\varepsilon_0\omega}\left[\varepsilon(\omega)q_\parallel\left(S_{zx} + \frac{q_\parallel}{q_\perp^0}S_{zz}\right)\right.$$
$$\left. + q_\perp\left(S_{xx} + \frac{q_\parallel}{q_\perp^0}S_{xz}\right)\right] = 0. \tag{88}$$

It is obvious that the mean value of the selvedge field, $\mathbf{E}^{\rm SE}(z)$, with a two-point (z, z') dyadic distribution function $\boldsymbol{\sigma}^{\rm SE}(z, z')$ necessarily must result in a much more complicated dispersion relation [Eq. (88)] than for a model with passive boundary conditions [Eq. (9)].

In a somewhat similar study, the electrodynamics of a QW sheet placed outside a sharp jellium surface was investigated a number of years ago [30,31].

A number of authors have attempted to investigate the plasmariton surface modes with active boundary conditions (yet with $J_z^S = 0$), treating the selvedge profile as an inhomogeneous plasma with a *local scalar conductivity*, $\sigma^{\rm SE}(z;\omega)$ [or, equivalently, a dielectric function $\varepsilon^{\rm SE}(z;\omega)$]. It appears, e.g., from the review article by Boardman [43], that also the local theory leads to a quite complicated dispersion relation of the SPM. In the framework of the local jellium model, the characteristic matrix

$$\mathbf{M}(q_\parallel,\omega) = \begin{pmatrix} 1 & \frac{ic}{\omega}\int_{\rm SE}\frac{q_\parallel^2-\varepsilon(z;\omega)\left(\frac{\omega}{c}\right)^2}{\varepsilon(z;\omega)}dz \\ -\frac{i\omega}{c}\int_{\rm SE}\varepsilon(z;\omega)dz & 1 \end{pmatrix} \tag{89}$$

relates the tangential components of the electric and magnetic fields on the two sides of the selvedge profiles. Thus, if the profile extends from $z=0$ to $z=d$, $E_x(d) = E_x(0) - M_{12}B_y(d)$, and $B_y(d) = B_y(0) - M_{21}E_x(d)$.

It must be emphasized that the local approximation breaks down when $q_\parallel\lambda^{\rm SE} \gtrsim 1$, where $\lambda^{\rm SE}$ is the characteristic length of the selvedge profile. In relation to the transverse dielectric function of Lindhard [44,45], this is the regime where the quantum parameter $z = q/(2k_F) \gtrsim 1$, k_F being the electron Fermi wave number. For $z \gtrsim 1$, electronic quantum interference effects play an essential role. It is these interference effects which are responsible for the Friedel oscillations in the selvedge profile.

Also the use of a z-dependent plasma frequency, $\omega_p(z)$, in itself gives rise to inconsistencies, e.g., light pulse reflection studies [45,46].

D. Self-field approach: Neglect of field retardation

The short length of the selvedge profile makes it possible to neglect the retardation in the field propagation across the selvedge. The vacuum propagator $\mathbf{G}(z-z')$ then can be replaced by its self-field (SF) part [31,39]:

$$\mathbf{g}_{\rm SF}(z-z') = -q_0^{-2}\delta(z-z')\hat{\mathbf{z}}\hat{\mathbf{z}}. \tag{90}$$

From Eq. (76), one then obtains a spatially local relation between the electric selvedge field, $\mathbf{E}_{\rm SF}^{\rm SE}(z)$, and the local surface current density $\mathbf{J}^{\rm SE}(z)$, namely,

$$\mathbf{E}_{\rm SF}^{\rm SE}(z) = \frac{1}{i\varepsilon_0\omega}J_z^{\rm SE}(z)\hat{\mathbf{z}}. \tag{91}$$

In the self-field approximation, the selvedge field is perpendicular to the plane of the surface, and the surface current density only has a z component.

The kernel in Eq. (80) now depends alone on electronic properties $[\mathbf{K}(z,z') \Rightarrow \mathbf{K}_{\rm SF}(z,z')]$. Hence,

$$\mathbf{K}_{\rm SF}(z,z') = \frac{1}{i\varepsilon_0\omega}\left[\sigma_{zx}^{\rm SE}(z,z')\hat{\mathbf{z}}\hat{\mathbf{x}} + \sigma_{zz}^{\rm SE}(z,z')\hat{\mathbf{z}}\hat{\mathbf{z}}\right]. \tag{92}$$

The absence of $\sigma_{xx}^{\rm SE}(z,z')$ and $\sigma_{xz}^{\rm SE}$ from the description implies that the related SPM dispersion relation is given by Eq. (88) setting $S_{xx} = S_{xz} = 0$. By writing the dispersion relation as follows:

$$q_\perp + \varepsilon_{\rm eff}(q_\parallel,\omega)q_\perp^0 = 0, \tag{93}$$

where

$$\varepsilon_{\rm eff}(q_\parallel,\omega) = \varepsilon(\omega)\left[1 + \frac{q_\parallel}{\varepsilon_0\omega}\left(S_{zx}(q_\parallel,\omega) + \frac{q_\parallel}{q_\perp^0}S_{zz}(q_\parallel,\omega)\right)\right], \tag{94}$$

it appears that its *form* is analogous to that of the passive case [Eq. (17)], just with the local dielectric function $\varepsilon(\omega)$ replaced by an effective one with spatial dispersion, $\varepsilon_{\rm eff}(q_\parallel,\omega)$. The spatial dispersion here stems from the selvedge alone.

The reader should compare this result to the dispersion relation

$$q_\perp + \varepsilon_T(q,\omega)q_\perp^0 = 0, \tag{95}$$

obtained for SPMs with (i) bulk spatial dispersion in the jellium, (ii) passive boundary conditions, and (iii) no L-mode contribution (the situation outside the strong L-T coupling region). If retardation is neglected in total ($c \to \infty$), Eq. (95) is reduced to

$$1 + \varepsilon_T(q_\parallel,\omega) = 0, \quad \text{ELECTROSTATIC.} \tag{96}$$

No magnetic field is present in the $c \to \infty$ limit, and the SPM dispersion relation takes the electrostatic form. This was to be expected since retardation plays a negligible role when the wave number (q) is much larger than the electron Fermi wave number (k_F). For electrostatic (ES) bulk plasmaritons,

$$\varepsilon_T(q,\omega) = 0, \quad \text{ES} \tag{97}$$

as we have discussed in Ref. [25], starting from Lindhard's transverse dielectric function. For plasmons (L plasmons), the corresponding formulas are $\varepsilon_L(q,\omega) = 0$ (bulk) and $1 + \varepsilon_L(q_\parallel,\omega) = 0$ (surface) [24]. These last two dispersion relations hold for all q ($q_\parallel$) due to the fact that light properties cannot enter longitudinal dynamics.

VII. SURFACE PLASMARITON DISPERSION RELATION IN THE FRAMEWORK OF A QUANTUM WELL MODEL

To carry out an explicit calculation of the dispersion relation given in Eq. (88), one needs a model for the field-unperturbed state of the jellium-vacuum system. Once the model has been chosen, one may, at least in principle, determine the related energy eigenstates and the associated (many-body) stationary-state electron wave functions. Below we shall limit ourselves to a single-electron approach and assume that the ion (background) potential is sharp and infinitely high. Although this model has a number of limitations (it excludes photoemission processes, e.g.), it illustrates the main principles of Sec. VI, and an analytic calculation can be carried through almost completely, provided the wave number of the field along the surface ($q_\parallel$) is much smaller than the electron Fermi wave number (k_F). In the most common situation where the relation of plasmariton surface modes to electromagnetic (∼optical) reflectivity is studied, the inequality $q_\parallel \ll k_F$ is justified.

A. One-electron conductivity tensor

It is known that the many-body expression for the microscopic conductivity tensor in the general three-dimensional case can be written in the form [39]

$$\boldsymbol{\sigma}(\mathbf{r},\mathbf{r}';\omega) = \frac{\hbar}{i}\sum_{I,J(\neq I)}\frac{P_J-P_I}{E_J-E_I}\frac{1}{\hbar\omega+E_J-E_I}\mathbf{J}_{I\to J}(\mathbf{r})\mathbf{J}_{J\to I}(\mathbf{r}') \quad (98)$$

in the space-frequency domain. The many-body stationary state Ψ_I (Ψ_J) is occupied with a probability P_I (P_J), and the associated eigenenergy is E_I (E_J). The quantity $\mathbf{J}_{I\to J}(\mathbf{r})$ [$\mathbf{J}_{J\to I}(\mathbf{r})$] denotes the transition current density from state I to state J (state J to I). The spatially nonlocal character of $\boldsymbol{\sigma}(\mathbf{r},\mathbf{r}';\omega)$ manifests itself through the fact that the transition current densities in Eq. (98) are taken at two (in general) different space points [$\mathbf{r},\mathbf{r}'$].

An important remark should be made here. No irreversible damping mechanisms (often characterized phenomenologically via a set of inverse relaxation times) have been included in Eq. (98). The SPM eigenmodes we seek belong to a closed system, and hence we should not include irreversible relaxation processes. In calculations where the gauge conserving diamagnetic part of $\boldsymbol{\sigma}(\mathbf{r},\mathbf{r}',\omega)$ is neglected, $\boldsymbol{\sigma}(\mathbf{r},\mathbf{r}',\omega)\to\infty$ for $\omega\to 0$, and in such simplified calculations it is necessary to include some kind of relaxation time to avoid the (unphysical) divergence of $\boldsymbol{\sigma}(\mathbf{r},\mathbf{r}',\omega)$ at $\omega=0$. BCS superconductors are excluded here because the vanishing of the paramagnetic part of $\boldsymbol{\sigma}(\mathbf{r},\mathbf{r}',\omega)$ implies that the conductivity tensor does diverge at $\omega=0$ (infinite conductivity). The sum of the para- and diamagnetic parts appear in Eq. (98), and it is obvious that there is no divergence in the $\omega\to 0$ limit.

From a fundamental theoretical point of view, a rigorous inclusion of relaxation processes first requires an identification of the most important microscopic scattering mechanism(s). For each these (impurities, phonons, etc.), a suitable (always cumbersome) calculation has to be carried out. Even in the framework of a QW surface model (Sec. VII D), such *ab initio* calculations are far beyond the scope of this paper. However, one might emphasize that perhaps a 2D calculation will be sufficient in the diamagnetic case (Sec. VII D 1), and a calculation similar to that carried out for two-level atoms may be sufficient, at least near the interlevel resonance frequency.

Experimental studies are most often linked to the relevant dispersion relation for the field, and relaxation phenomena are in many cases included via a phenomenologically introduced relaxation time (τ). In our numerical calculations for the one-level diamagnetic intraband and the two-level paramagnetic interband transitions, to be presented in Sec. VII E, one might to some extent include (all) irreversible relaxation processes by replacing ω by $\omega+i/\tau_{\text{dia}}$ and $\omega+i/\tau_{\text{para}}$ in the relevant dispersion relations [Eqs. (125) and (128), with $\mathcal{N}_0$ and β given by Eqs. (129) and (136)].

Let us now turn our attention toward the one-electron approximation. For flat adjacent jellium-vacuum systems, we make the ansatz

$$\psi_n(\mathbf{r}) = \frac{1}{2\pi}\exp(i\mathbf{k}_\parallel\cdot\mathbf{r})u_n(z), \quad (99)$$

$\mathbf{k}_\parallel$ being an electron wave vector along the surface. The ansatz in Eq. (99) is the relevant one here, because we assume that the self-consistent potential energy alone is a function of z, $U(z)$. The central quantity for the analysis below is the mixed conductivity tensor, $\boldsymbol{\sigma}(\mathbf{q}_\parallel,\omega;z,z')$. With assumed spin degeneracy (factor of 2 in front of the summation sign in the subsequent equation) [39],

$$\boldsymbol{\sigma}(\mathbf{q}_\parallel,\omega;z,z') = \frac{2\hbar}{i}\sum_{n,n'}\int_{-\infty}^{\infty}\left\{\frac{f_0\left(\varepsilon_n+\frac{\hbar^2}{2m}k_\parallel^2\right)-f_0\left(\varepsilon_{n'}+\frac{\hbar^2}{2m}|\mathbf{k}_\parallel+\mathbf{q}_\parallel|^2\right)}{\varepsilon_n-\varepsilon_{n'}+\frac{\hbar^2}{2m}k_\parallel^2-\frac{\hbar^2}{2m}|\mathbf{k}_\parallel+\mathbf{q}_\parallel|^2}\frac{1}{\hbar\omega+\varepsilon_n-\varepsilon_{n'}+\frac{\hbar^2}{2m}k_\parallel^2-\frac{\hbar^2}{2m}|\mathbf{k}_\parallel+\mathbf{q}_\parallel|^2}\right.$$
$$\left.\times\,\mathbf{j}_{n'\to n}(\mathbf{k}_\parallel,\mathbf{k}_\parallel+\mathbf{q}_\parallel;z)\mathbf{j}_{n\to n'}(\mathbf{k}_\parallel,\mathbf{k}_\parallel+\mathbf{q}_\parallel;z')\right\}\frac{d^2k_\parallel}{(2\pi)^2}, \quad (100)$$

where

$$\mathbf{j}_{n\to n'}(\mathbf{k}_\parallel,\mathbf{k}_\parallel+\mathbf{q}_\parallel;z') = -\frac{e\hbar}{2im}\left\{i(2\mathbf{k}_\parallel+\mathbf{q}_\parallel)u^*_{n'}(z')u_n(z')+\hat{\mathbf{z}}\left[u^*_{n'}(z')\frac{du_n(z')}{dz'}-u_n(z')\frac{du^*_{n'}(z')}{dz'}\right]\right\} \quad (101)$$

is the electron [charge: $-e$, mass: m] transition current density from state n to state n', evaluated at z. An analogous expression for $\mathbf{j}_{n'\to n}(\mathbf{k}_\parallel,\mathbf{k}_\parallel+\mathbf{q}_\parallel;z)$ follows from Eq. (101), making the interchanges $n\to n'$, $n'\to n$, and $z'\to z$. The quantity $f_0(E_n)$ [$f_0(E_{n'})$] is the Fermi-Dirac distribution function for $E_n=\varepsilon_n+[\hbar^2/(2m)]k_\parallel^2$ [$E_{n'}=\varepsilon'_{n'}+[\hbar^2(2m)]|\mathbf{k}_\parallel+\mathbf{q}_\parallel|^2$] ε_n [$\varepsilon_{n'}$] being the nth eigenenergy belonging to the one-dimensional time-independent Schrödinger equation:

$$\left[-\frac{\hbar^2}{2m}\frac{d^2}{dz^2}+U(z)-\varepsilon_n\right]u_n(z)=0. \quad (102)$$

With assumed spin degeneracy, f_0 is normalized to half the number of electrons.

For $q_\parallel\ll k_F$, one just needs the expression for $\boldsymbol{\sigma}(\mathbf{q}_\parallel,\omega;z,z')$ in the small $\mathbf{q}$ limit, viz.,

$$\boldsymbol{\sigma}(\mathbf{q}_\parallel\to 0,\omega;z,z') = \frac{2\hbar}{i}\sum_{n,n'}\int_{-\infty}^{\infty}\frac{f_0\left(\varepsilon_n+\frac{\hbar^2}{2m}k_\parallel^2\right)-f_0\left(\varepsilon_{n'}+\frac{\hbar^2}{2m}k_\parallel^2\right)}{(\varepsilon_n-\varepsilon_{n'})(\hbar\omega+\varepsilon_n-\varepsilon_{n'})}$$
$$\times\,\mathbf{j}_{n'\to n}(2\mathbf{k}_\parallel;z)\mathbf{j}_{n\to n'}(2\mathbf{k}_\parallel;z')\frac{d^2k_\parallel}{(2\pi)^2}, \quad (103)$$

where

$$\mathbf{j}_{n'\to n}(2\mathbf{k}_\parallel;z) = -\frac{e\hbar}{2im}\left\{2i\mathbf{k}_\parallel u_n^*(z)u_n'(z) + \hat{\mathbf{z}}\left[u_n^*(z)\frac{du_n'(z)}{dz} - u_n'(z)\frac{du_n^*(z)}{dz}\right]\right\}. \quad (104)$$

B. The diagonal form of $\sigma(\mathbf{q}_\parallel, \omega; z, z')$

In the integration over $\mathbf{k}_\parallel$ appears the Fermi-Dirac distribution function, which is a function of $k_\parallel^2 = k_{\parallel,x}^2 + k_{\parallel,y}^2$, and dyadic products proportional to $\mathbf{k}_\parallel\mathbf{k}_\parallel$ [$\mathbf{k}_\parallel = k_{\parallel,x}\hat{\mathbf{x}} + k_{\parallel,y}\hat{\mathbf{y}}$], $\mathbf{k}_\parallel\hat{\mathbf{z}}$, $\hat{\mathbf{z}}\mathbf{k}_\parallel$, and $\hat{\mathbf{z}}\hat{\mathbf{z}}$. Integrals [$\int_{-\infty}^{\infty}(\dots)d^2k_\parallel$] with integrands uneven in $k_{\parallel,x}$ or $k_{\parallel,y}$ vanish, leaving one with the generally nonvanishing elements σ_{xx}, σ_{yy}, and σ_{zz}.

For the plasmariton case, the conductivity tensor (in 2×2-matrix form) hence is diagonal in the limit $\mathbf{q}_\parallel = q_\parallel\hat{\mathbf{x}} \to \mathbf{0}$, i.e.,

$$\sigma(\mathbf{q}_\parallel \to 0, \omega; z, z') = \begin{pmatrix}\sigma_{xx}(\omega; z, z') & 0\\ 0 & \sigma_{zz}(\omega, z, z')\end{pmatrix}. \quad (105)$$

Using the explicit expression for the Fermi-Dirac distribution function (normalized to half the number of electrons), viz.,

$$f_0(E_n) = \left[1 + \exp\left(\frac{\varepsilon_n - \mu}{kT}\right)\exp\left(\frac{\hbar^2 k_\parallel^2}{2mkT}\right)\right]^{-1}, \quad (106)$$

where μ, k, T are the chemical potential, the Boltzmann constant, and the absolute temperature, respectively, the $\mathbf{k}_\parallel$ integrals belonging to σ_{xx} and σ_{zz} are ($\varepsilon = \varepsilon_n$ and $\varepsilon_{n'}$)

$$\begin{aligned}F_{xx}(\varepsilon) &\equiv \int_{-\infty}^{\infty} f_0\left(\varepsilon + \frac{\hbar^2 k_\parallel^2}{2m}\right)k_{\parallel,x}^2\frac{d^2k_\parallel}{(2\pi)^2}\\ &= \frac{1}{2\pi}\left(\frac{mkT}{\hbar^2}\right)^2\int_0^\infty \frac{xdx}{\left[1+\exp\left(\frac{\varepsilon-\mu}{kT}\right)e^x\right]}\\ &\xrightarrow[T\to 0]{} \begin{cases}\frac{1}{4\pi}\left(\frac{m}{\hbar^2}\right)^2(\varepsilon_F - \varepsilon)^2; & \varepsilon < \varepsilon_F\\ 0; & \varepsilon > \varepsilon_F\end{cases}\end{aligned} \quad (107)$$

and

$$\begin{aligned}F_{zz}(\varepsilon) &= \int_{-\infty}^{\infty} f_0\left(\varepsilon + \frac{\hbar^2 k_\parallel^2}{2m}\right)\frac{d^2k_\parallel}{(2\pi)^2}\\ &= \frac{1}{2\pi}\frac{mkT}{\hbar^2}\ln\left[1+\exp\left(\frac{\varepsilon-\mu}{kT}\right)\right]\\ &\xrightarrow[T\to 0]{} \begin{cases}\frac{1}{2\pi}\frac{m}{\hbar^2}(\varepsilon - \varepsilon_F); & \varepsilon < \varepsilon_F\\ 0; & \varepsilon > \varepsilon_F.\end{cases}\end{aligned} \quad (108)$$

With the $\mathbf{k}_\parallel$ integrations carried out, the one-electron conductivity tensor takes the following dyadic form:

$$\begin{aligned}&\sigma(\mathbf{q}_\parallel \to 0, \omega; z, z')\\ &= \frac{2\hbar}{i}\left(\frac{e\hbar}{2m}\right)^2\sum_{n,n'}\frac{1}{(\varepsilon_n - \varepsilon_{n'})(\hbar\omega + \varepsilon_n - \varepsilon_{n'})}\\ &\times\{4P_{xx}[F_{xx}(\varepsilon_n) - F_{xx}(\varepsilon_{n'})]\hat{\mathbf{x}}\hat{\mathbf{x}}\\ &-P_{zz}[F_{zz}(\varepsilon_n) - F_{zz}(\varepsilon_{n'})]\hat{\mathbf{z}}\hat{\mathbf{z}}\},\end{aligned} \quad (109)$$

where

$$P_{xx} = u_n^*(z)u_{n'}(z)u_{n'}^*(z')u_n(z') \quad (110)$$

and

$$\begin{aligned}P_{zz} &= \left[u_n^*(z)\frac{du_{n'}(z)}{dz} - u_{n'}(z)\frac{du_n^*(z)}{dz}\right]\\ &\times\left[u_{n'}^*(z')\frac{du_n(z')}{dz'} - u_n(z')\frac{du_{n'}^*(z)}{dz'}\right].\end{aligned} \quad (111)$$

C. Electric-dipole conductivity tensor in the low-temperature limit

As a first step toward a calculation of the selvedge tensor $\mathbf{S}$ [given in Eq. (86)] for a specific model, let us determine the tensor

$$\mathbf{S}^0 \equiv \int_{-\infty}^{\infty}\sigma(\mathbf{q}_\parallel \to 0, \omega, z, z')dz'dz \quad (112)$$

in the low-temperature limit. Since

$$\int_{-\infty}^{\infty}P_{xx}(z, z')dz'dz = \delta_{n,n'} \quad (113)$$

due to the orthonormality of the stationary state eigenfunctions, and

$$\begin{aligned}&[F_{xx}(\varepsilon_n) - F_{xx}(\varepsilon_{n'})]_{T\to 0}\\ &= \frac{1}{4\pi}\left(\frac{m}{\hbar^2}\right)^2(\varepsilon_F - \varepsilon_n)^2\Theta(\varepsilon_F - \varepsilon_n)\\ &-(\varepsilon_F - \varepsilon_{n'})^2\Theta(\varepsilon_F - \varepsilon_{n'}),\end{aligned} \quad (114)$$

where $\Theta(\varepsilon_F - \varepsilon_{n'})$ is the Heaviside step function, elementary calculations give the following result for the xx component of $\mathbf{S}^0$ for $T \to 0$:

$$S_{xx}^0(\omega|T\to 0) = \frac{e^2}{\pi i\hbar^2}\frac{1}{\omega}\sum_n(\varepsilon_n - \varepsilon_F)\Theta(\varepsilon_F - \varepsilon_n), \quad (115)$$

possibly with $\sum_n(\varepsilon_n - \varepsilon_F) = -(2/5)\varepsilon_F n$ inserted ($n = N/V$: number of electrons per unit volume).

To determine the zz component of $\mathbf{S}^0$, we utilize the well-known result (and an analogous one with n and n' interchanged)

$$\begin{aligned}&\int_{-\infty}^{\infty}\left[u_n^*(z)\frac{du_{n'}(z)}{dz} - u_{n'}(z)\frac{du_n^*(z)}{dz}\right]dz\\ &= \frac{2m}{\hbar^2}(\varepsilon_{n'} - \varepsilon_n)P_{n'\to n},\end{aligned} \quad (116)$$

where

$$P_{n'\to n} = \int_{-\infty}^{\infty}u_n^*(z)zu_{n'}(z)dz \quad (117)$$

is the matrix element connected with an electric-dipole transition form state n' to state n ($n' \to n$). Hence,

$$\begin{aligned}&\int_{-\infty}^{\infty}P_{zz}(z, z')dz'dz\\ &= \left(\frac{2m}{\hbar^2}\right)^2(\varepsilon_{n'} - \varepsilon_n)(\varepsilon_n - \varepsilon_{n'})P_{n'\to n}P_{n\to n'}.\end{aligned} \quad (118)$$

In the low-temperature limit:

$$H_{zz}(\varepsilon_n, \varepsilon_{n'}) \equiv [F_{zz}(\varepsilon_n) - F_{zz}(\varepsilon_{n'})]_{T\to 0}$$
$$= \frac{1}{2\pi}\frac{m}{\hbar^2}[(\varepsilon_n - \varepsilon_{n'})\Theta(\varepsilon_F - \varepsilon_n)$$
$$\Theta(\varepsilon_F - \varepsilon_{n'})$$
$$+ (\varepsilon_n - \varepsilon_F)\Theta(\varepsilon_F - \varepsilon_n)\Theta(\varepsilon_{n'} - \varepsilon_F)$$
$$+ (\varepsilon_{n'} - \varepsilon_F)\Theta(\varepsilon_n - \varepsilon_F)\Theta(\varepsilon_F - \varepsilon_{n'})]. \quad (119)$$

By gathering the information in Eqs. (110), (113), (118), and (119), one obtains

$$S^0_{zz}(\omega|T \to 0)$$
$$= \frac{2e^2}{i\hbar}\sum_{n,n'} H_{zz}(\varepsilon_n, \varepsilon_{n'})\frac{\varepsilon_n - \varepsilon_{n'}}{\hbar\omega + \varepsilon_n - \varepsilon_{n'}}P_{n'\to n}P_{n\to n'}. \quad (120)$$

Although the result obtained for $\mathbf{S}^0 = S^0_{xx}\hat{\mathbf{x}}\hat{\mathbf{x}} + S^0_{zz}\hat{\mathbf{z}}\hat{\mathbf{z}}$ is extremely simple for $T \to 0$, one cannot proceed to a determination of the selvedge tensor $\mathbf{S}$ [Eq. (86)] unless a specific model is chosen for the field-unperturbed state of the adjacent vacuum-jellium system.

D. Quantum-well surface current density

In the following, we shall study the SPM eigenmodes in a model where the surface current density originates in a QW film deposited on the jellium surface. From a qualitative point of view, the QW film thus acts as a kind of selvedge. [$\boldsymbol{\sigma}^{\mathrm{SE}} \sim \boldsymbol{\sigma}^{\mathrm{QW}}$]. In the $\mathbf{q}_\parallel \to 0$ limit, we start from a model conductivity tensor of the form

$$\boldsymbol{\sigma}(\omega; z, z') = \boldsymbol{\sigma}^{\mathrm{QW}}(\omega; , z, z')\Theta(-z)\Theta(z+d) + \sigma^{\mathrm{J}}(\omega)\mathbf{U}\Theta(z). \quad (121)$$

In line with our previous assumption (Sec. II), we consider an isotropic and spatially nondispersive semi-infinite jellium (J) with $\sigma^J(\omega) = i\varepsilon_0\omega_p^2/\omega$ [corresponding to $\varepsilon^{\mathrm{J}}(\omega) = 1 - (\omega_p/\omega)^2$], and we neglect the selvedge profile. Instead the active surface current density is associated to a QW with infinitely high potential barriers located at $z = -d$ and $z = 0$. Inside the QW, the potential is flat. The infinitely high barrier assumed at $z = 0$ implies that electrons are not exchanged between the QW and J parts.

In free-electron-like (∼jellium) semiconductors (like InSb and GaAs), it is possible to change the relative importance of S^{QW}_{xx} and S^{QW}_{zz}. The relative importance may be changed by displacing the Fermi level via doping.

1. Diamagnetic response

It appears from Eq. (115) that the xx component of the QW $\mathbf{S}$-matrix is given by

$$S^{\mathrm{QW}}_{xx}(\omega|T \to 0) = \frac{e^2}{\pi i\hbar^2}\frac{1}{\omega}\sum_n(\varepsilon_n - \varepsilon_F)\Theta(\varepsilon_F - \varepsilon_n) \quad (122)$$

in the low-temperature limit. The energies $\varepsilon_n \equiv \varepsilon^{\mathrm{QW}}_n$ entering Eq. (122) are those of the QW film. For $q_\parallel = 0$, there are no electric-dipole transitions parallel to the jellium-vacuum interface, remembering that $n = n'$ [Eq. (115)]. Physically, this means that S^{QW}_{xx} originates alone in dynamic diamagnetism, letting the electrons stay in the given ε_n level. The general trend is that the diamagnetic contribution to the $\mathbf{S}$ matrix tends to dominate in the low-frequency region [cf. the ω^{-1} factor in Eq. (122)]. Although, S^{QW}_{zz} does not vanish for small ω, S^{QW}_{zz} gives a frequency-independent term for $\omega \ll |\varepsilon_n - \varepsilon_{n'}|/\hbar$, $\forall n, n'$. In the case where the film thickness is so small that there effectively is only one bound level (below the Fermi energy)—a possibility for finite barrier height, yet so high that electron flow between the QW and jellium is negligible—one may take $S^0_{zz}(\omega|T \to 0) \approx 0$ for small frequencies.

In view of the discussion of the dynamic boundary conditions in Sec. II, it appears that the active surface current density flows parallel to the interface if only diamagnetic effects are included in the analysis. The associated SPM dispersion relation follows from Eq. (88), setting $S^{\mathrm{QW}}_{xz} = S^{\mathrm{QW}}_{zx} = S^{\mathrm{QW}}_{zz} = 0$. With the abbreviation

$$\alpha = \frac{e^2}{\pi\hbar^2}\sum_n(\varepsilon_F - \varepsilon_n)\Theta(\varepsilon_F - \varepsilon_n), \quad (123)$$

its implicit form is given by

$$q_\perp + \varepsilon(\omega)q^0_\perp + \frac{i\alpha}{\varepsilon_0\omega^2}q_\perp q^0_\perp = 0. \quad (124)$$

For evanescent solutions, we utilize $q_\perp = i\kappa_\perp$ and $q^0_\perp = i\kappa^0_\perp$ and obtain

$$\kappa_\perp + \varepsilon(\omega)\kappa^0_\perp - \frac{\alpha}{\varepsilon_0\omega^2}\kappa_\perp\kappa^0_\perp = 0. \quad (125)$$

2. Paramagnetic response

Another extreme occurs if the diamagnetic response is negligible. It appears from previous studies that this can be a good approximation in relation to certain optical reflection studies [30,31] and in small-hole diffraction from microscopic holes in two (or few) level QW screens [40,47,48]. Setting $S^{\mathrm{QW}}_{xz} = S^{\mathrm{QW}}_{zx} = S^{\mathrm{QW}}_{xx} = 0$, the dispersion relation in Eq. (88) is reduced to

$$q_\perp + \varepsilon(\omega)q^0_\perp - \frac{i\varepsilon(\omega)}{\varepsilon_0\omega}\beta(\omega)q^2_\parallel = 0, \quad (126)$$

where

$$\beta(\omega) = \frac{2e^2}{\hbar}\sum_{n,n'} H^{\mathrm{QW}}_{zz}(\varepsilon_n, \varepsilon_{n'})\frac{\varepsilon_n - \varepsilon_{n'}}{\hbar\omega + \varepsilon_n - \varepsilon_{n'}}P_{n'\to n}P_{n\to n'}. \quad (127)$$

The quantity $H^{\mathrm{QW}}_{zz}(\varepsilon_n, \varepsilon_{n'})$ is given formally by Eq. (119), remembering that one must take $\varepsilon_n = \varepsilon^{\mathrm{QW}}_n$ and $\varepsilon_{n'} = \varepsilon^{\mathrm{QW}}_{n'}$. For evanescent solutions, we arrive at the following dispersion relation:

$$\kappa_\perp + \varepsilon(\omega)\kappa^0_\perp - \frac{\varepsilon(\omega)}{\varepsilon_0\omega}\beta(\omega)q^2_\parallel = 0. \quad (128)$$

E. Numerical results

Below we calculate and discuss numerical results for the dia- and paramagnetic cases. Material parameters for n-InSb are used (see Fig. 2 caption), and it is assumed that the QW barrier is infinitely high. We limit ourselves to a QW film so thin that only the two lowest-lying electron energy levels need to be included in the relevant optical frequency range.

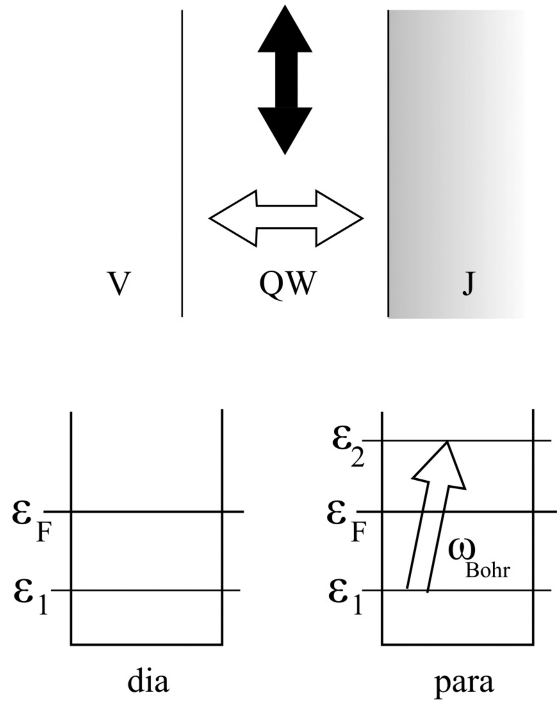

FIG. 1. Schematic illustration of a quantum well (QW) squeezed between vacuum (V) and jellium (J). For a one-level (ε_1) QW, where $\varepsilon_1 < \varepsilon_F$ (Fermi energy), the current flow (black double arrow) is everywhere parallel to the surface plane whereas a two-level QW, with $\varepsilon_1 < \varepsilon_F < \varepsilon_2$, predominantly is perpendicular to the interface (white double arrow), for optical frequencies in the vincinity of the Bohr transistion frequency, $\omega_{\mathrm{Bohr}} = (\varepsilon_2 - \varepsilon_1)/\hbar$.

By suitable (n-type) doping, the Fermi is located between the two levels. A sketch of the two-level QW model belonging to the dia- and paramagnetic surface current densities is shown in Fig. 1.

1. One-level diamagnetic case

By introduction of the surface electron density [42],

$$\mathcal{N}_0 = \frac{m}{\pi\hbar^2}\sum_n(\varepsilon_F - \varepsilon_n)\Theta(\varepsilon_F - \varepsilon_n), \tag{129}$$

which for only one level (ε_1) below the Fermi energy becomes $\mathcal{N}_0 = m(\varepsilon_F - \varepsilon_1)/(\pi\hbar^2)$, the dispersion relation in Eq. (125) can be rewritten in the form

$$\kappa_\perp + \varepsilon(\omega)\kappa_\perp^0 - \left(\frac{\Omega_{\mathrm{dia}}}{\omega}\right)^2\kappa_\perp\kappa_\perp^0 = 0. \tag{130}$$

The quantity

$$\Omega_{\mathrm{dia}} = \left(\frac{\mathcal{N}_0 e^2}{m\varepsilon_0}\right)^{1/2} \tag{131}$$

may be named a sheet plasma frequency because of its form, although the dimension of Ω_{dia} is a frequency divided by the square root of a wave number.

Figure 2 shows the SPM dispersion relation obtained from Eq. (130) plotted in normalized form, i.e., ω/ω_p as a function of $q_\parallel c/\omega_p$. At small wave numbers, the dispersion relation becomes identical to the Fano mode for a passive boundary.

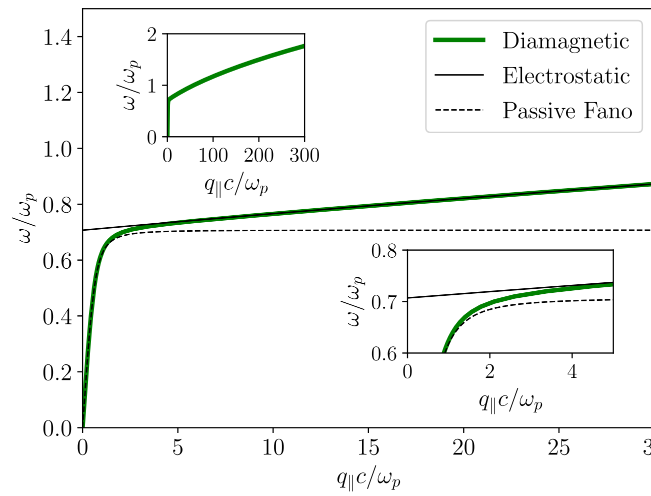

FIG. 2. Diamagnetic dispersion relation (thick green line) on normalized form (i.e., ω/ω_p versus $cq_\parallel/\omega_p$) for a surface plasmariton with an active boundary in the form of a one-level quantum well (assuming infinitely high barriers). For small wave numbers, the dispersion relation coincides with the passive boundary Fano branch (thin dashed line). This branch approaches the surface plasma frequency, $\omega/\omega_p = 1/\sqrt{2}$ for $q_\parallel \to \infty$. At high wave numbers, the dispersion relation coincides with that obtained in an electrostatic ($c \to \infty$) approximation (thin black line). For $q_\parallel = 0, \omega/\omega_p = 1/\sqrt{2}$ in the electrostatic approximation. The transition region between the Fano and electrostatic branches is plotted in the inset to the right. The numerical plots in Figs. 2–4 are for a semiconducting n-InSb plasma, using the following data: $m = 0.015m_0$ (m_0: free-electron mass) and $n = 4 \times 10^{18}$ cm^{-3}. The width of the quantum well active boundary is $d = 10$ nm.

The Fano mode approaches the surface plasma frequency $\omega_{pS} = \omega_p/\sqrt{2}$ from below for $q_\parallel c/\omega_p \to \infty$, whereas the diamagnetic dispersion relation (active boundary) crosses ω_{pS}, as shown. It appears that most of the dispersion relations lying above ω_{pS} is well represented by an electrostatic approximation ($c \to \infty$). In the electrostatic regime, where $\kappa_\perp^0 \to q_\parallel$, $\kappa_\perp \to q_\parallel$, Eq. (130) is reduced to

$$q_\parallel^{\mathrm{ES}}(\omega) = \frac{2\omega^2 - \omega_p^2}{\Omega_{\mathrm{dia}}^2}. \tag{132}$$

In the electrostatic approximation, the decay constants are the same in the plasma and the vacuum, viz., $\kappa_\perp = \kappa_\perp^0 = q_\parallel$; cf. Eqs (25) and (32). This means that the jellium properties play no role: The diamagnetic sheet current density is placed in vacuum, essentially. In Sec. V III, we describe how this finding relates to a SPM quasiparticle picture.

Before proceeding to the paramagnetic case, it is worth mentioning that the calculation of $q_\parallel = q_\parallel(\omega)$ (or its inverse) is not without numerical pitfalls if the expressions for $\kappa_\perp^0$ [Eq. (25)] and $\kappa_\perp$ [Eq. (32)] are inserted into Eq. (130) directly. If one instead, for a given ω, determines the crossing point of the $\kappa_\perp^0 = \kappa_\perp^0(\kappa_\perp)$, viz.,

$$\kappa_\perp^0 = \frac{\kappa_\perp}{\left(\frac{\Omega_{\mathrm{dia}}}{\omega}\right)^2\kappa_\perp - \varepsilon(\omega)}, \tag{133}$$

$$\kappa_\perp^0 = \left[\kappa_\perp^2 - \left(\frac{\omega_p}{c}\right)^2\right]^{1/2}, \tag{134}$$

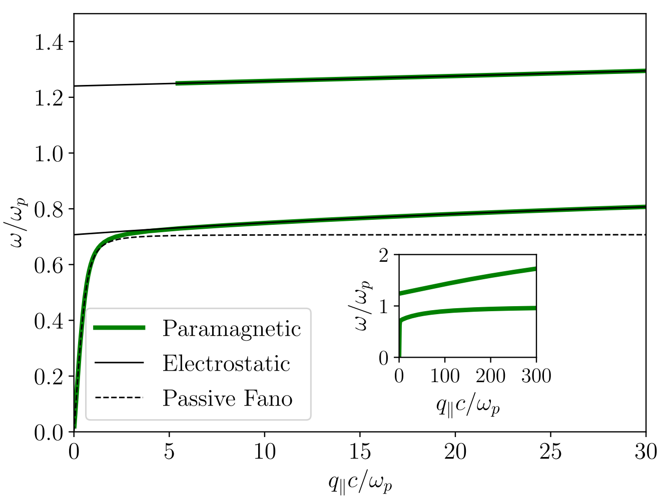

FIG. 3. Paramagnetic dispersion relation with its two branches (thick green lines) in normalized form (i.e., ω/ω_p versus $cq_\parallel/\omega_p$) for a surface plasmariton with an active boundary in the form of a two-level quantum well (infinitely high barriers assumed). As in Fig. 2, the lower branch is well represented by the passive Fano and electrostatic models at low and high wave numbers, respectively. The upper branch is essentially electrostatic, yet with a low wave number cutoff at $cq_\parallel/\omega_p \simeq 5.4$. At $q_\parallel = 0$, $\omega/\omega_p = \omega_{\mathrm{Bohr}}/\omega_p \simeq 1.25$. The numerical calculations are for semiconducting n-InSb (data as for Fig. 2).

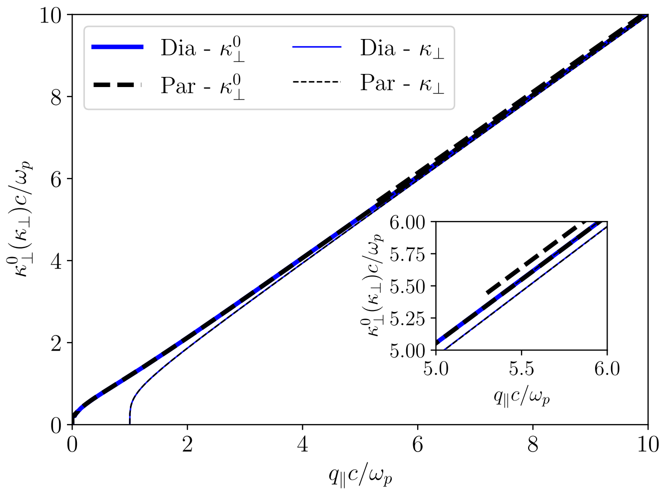

FIG. 4. Surface plasmariton decay constants in vacuum ($\kappa_\perp^0$) and in the jellium ($\kappa_\perp$) as a function of the normalized wave number along the surface ($cq_\parallel/\omega_p$). Results are presented for both the diamagnetic and paramagnetic cases, for which dispersion relations are shown in Figs. 2 and 3. For $q_\parallel \to \infty$, $\kappa_\perp^0 \to q_\parallel$ and $\kappa_\perp \to q_\parallel$, giving a straight line $\kappa_\perp = \kappa_\perp^0 = q_\parallel$. The value $q_\parallel^{-1}$ in the electrostatic region corresponds to the 1D confinement of the T-photon source (see also Figs. 5 and 6).

and thereafter calculates $q_\parallel(\omega)$ from $q_\parallel = [(\kappa_\perp^0)^2 + (\omega/c)^2]^{1/2}$, pitfalls are avoided—an analogous numerical scheme we employed in the paramagnetic case.

2. *Two-level paramagnetic case*

To determine the paramagnetic dispersion relation for a two-level QW ($\varepsilon_1 < \varepsilon_F < \varepsilon_2$), one first determines $\beta(\omega)$ from Eq. (127). A straightforward calculation gives from Eq. (119)

$$H_{ZZ}^{\mathrm{QW}}(\varepsilon_2, \varepsilon_1) = H_{ZZ}^{\mathrm{QW}}(\varepsilon_1, \varepsilon_2) = \frac{m}{2\pi\hbar^2}(\varepsilon_1 - \varepsilon_F), \tag{135}$$

and then

$$\beta(\omega) = \frac{2me^2}{\pi\hbar^3}|P_{1\to 2}|^2(\varepsilon_1 - \varepsilon_F)\frac{(\varepsilon_2 - \varepsilon_1)^2}{(\varepsilon_2 - \varepsilon_1)^2 - (\hbar\omega)^2}. \tag{136}$$

By inserting this expression for $\beta(\omega)$ into Eq. (128), the numerical calculation of the paramagnetic dispersion relation can be carried out. Hence, utilizing that $q_\parallel^2 = (\kappa_\perp^0)^2 + (\omega/c)^2$ one can employ the same numerical scheme as in the diamagnetic case.

The normalized paramagnetic dispersion relation [ω/ω_p versus $q_\parallel c/\omega_p$] is shown in Fig. 3. The dispersion relation has two branches. The lower branch is qualitatively similar to the diamagnetic dispersion relation. The high-wave-number part of the lower branch and the entire upper branch are well described by the electrostatic approximation, namely,

$$q_\parallel^{\mathrm{ES}}(\omega) = \frac{2\varepsilon_0\omega}{\beta(\omega)}\frac{\omega^2 - \omega_{pS}^2}{\omega^2 - \omega_p^2}. \tag{137}$$

For $q_\parallel \Rightarrow 0$, the two electrostatic branches approach the points $\omega = \omega_{pS}$ and $\omega = \omega_{\mathrm{Bohr}} = (\varepsilon_2 - \varepsilon_1)/\hbar$ ($\omega_{\mathrm{Bohr}}/\omega_p \approx$ 1.25, here). There is a low wave number cutoff in the upper branch, as the reader may infer from the dispersion relation in Eq. (128), since $\beta(\omega) > 0$ for $\omega > \omega_B$.

In Fig. 4, the decay constants $\kappa_\perp^0$ and $\kappa_\perp$ are shown as a function of $q_\parallel$, all three quantities being multiplied by the factor c/ω_p. The plots give a qualitative expression of how good the electrostatic approximation $\kappa_\perp^0 = \kappa_\perp = q_\parallel$ is.

VIII. CONNECTION TO THE PLASMARITON QUASIPARTICLE PICTURE

A. Remarks on the bulk plasmariton quasiparticle theory

In a recent paper on the wave-mechanical and second-quantized theories of bulk plasmaritons [25], we developed a Hamiltonian quasiparticle description in which the transverse part of the microscopic displacement field, multiplied by a factor of minus one, viz.,

$$\mathbf{M} \equiv -\mathbf{D}_T = -(\varepsilon_0\mathbf{E}_T + \mathbf{P}_T), \tag{138}$$

acts as a canonical field momentum. The time evolution of the jellium polarization ($\mathbf{P}$) which is transversely polarized ($\mathbf{P} = \mathbf{P}_T$) in the plasmariton case becomes equivalent to that of an essentially charged harmonic oscillator. The transverse electric field is the sum of retarded (R) and self-field (SF) parts,

$$\mathbf{E}_T = \mathbf{E}_T^R + \mathbf{E}_T^{\mathrm{SF}}, \tag{139}$$

since $\mathbf{D}_T$ relates to the *free* field momentum, $\mathbf{D}_T$ must be given by

$$\mathbf{D}_T = \varepsilon_0\mathbf{E}_T^R. \tag{140}$$

A combination of Eqs. (138)–(140) then shows that the transverse electric self-field is

$$\mathbf{E}_T^{\mathrm{SF}} = -\frac{1}{\varepsilon_0}\mathbf{P}_T. \tag{141}$$

One may write the relation between the transverse electric self field and the transverse polarization as $\mathbf{E}_T^{\mathrm{SF}} = -\mathbf{P}_T/(n\varepsilon_0)$, with $n = 1$. The positive integer relates to the dimensionality of the field confinement (here 1D: $n = 1$, for the plasmariton field). In the atomic case, where one has 3D confinement, $n = 3$, and thus $\mathbf{E}_T^{\mathrm{SF}} = -\mathbf{P}_T/(3\varepsilon_0)$; cf. the propagator theory describing the spatial confinement of quantized light emitted from a single atom [38].

In the Hamiltonian description based on $\mathbf{D}_T$, a term

$$\mathcal{H}_{\mathrm{tied}} \equiv \frac{\mathbf{P}_T^2}{2\varepsilon_0} = \frac{\varepsilon_0}{2}\left(\mathbf{E}_T^{\mathrm{SF}}\right)^2, \tag{142}$$

appears in the Hamiltonian density. This term, which only depends on the polarization density variables, is to be grouped with the oscillator part of the total Hamiltonian density. $\mathcal{H}_{\mathrm{tied}}$ describes the T-photon cloud tied (attached) to the plasmariton quasiparticle [25].

In the $\mathbf{D}_T$ formalism, the interaction (I) Hamiltonian density is given by

$$\mathcal{H}_I = \frac{1}{\varepsilon_0}\mathbf{M}\cdot\mathbf{P}_T = \varepsilon_0\mathbf{E}_T^R\cdot\mathbf{E}_T^{\mathrm{SF}}, \tag{143}$$

and hence relates to the scalar product between the retarded and self-field parts of the transverse electric field. In Sec. IX, we shall study the SPM's interaction with an retarded external field, $\mathbf{E}_{\mathrm{ext}}^R$.

B. Surface plasmariton self-field

In the covariant formalism, the transverse vector potential is invariant against gauge transformation within the Lorenz gauge, and more generally the same in all gauges. This means that the quantization schemes for $\mathbf{A}_T(z;\omega)$ and $\mathbf{E}_T(z;\omega) = i\omega\mathbf{A}_T(z,\omega)$ essentially are the same; cf. Eq. (37).

To obtain the transverse self-field of the SPM field, let us return Eqs. (10) and (11) in the form these take in the evanescent regime ($q_\perp^0 \Rightarrow i\kappa_\perp^0$, $q_\perp = i\kappa_\perp$). Multiplied by the plane-wave factor $\exp(iq_\parallel x)$, one has

$$\mathbf{E}_T^V(x,z;\omega) = A_V\left(\hat{\mathbf{x}} - i\frac{q_\parallel}{\kappa_\perp^0}\hat{\mathbf{z}}\right)e^{\kappa_\perp^0 z}e^{iq_\parallel x}, \tag{144}$$

$$\mathbf{E}_T^J(x,z;\omega) = A_J\left(\hat{\mathbf{x}} + i\frac{q_\parallel}{\kappa_\perp}\hat{\mathbf{z}}\right)e^{-\kappa_\perp z}e^{iq_\parallel x}. \tag{145}$$

The nonretarded parts of Eqs. (144) and (145) constitute the transverse self-field of the SPM field. Since $\kappa_\perp^0 \to q_\parallel$ and $\kappa_\perp \to q_\parallel$ for $c \to \infty$, one gets

$$\mathbf{E}_T^{V,\mathrm{SF}}(x,z) = A_V(\hat{\mathbf{x}} - i\hat{\mathbf{z}})e^{q_\parallel(ix+z)}, \tag{146}$$

$$\mathbf{E}_T^{J,\mathrm{SF}}(x,z) = A_J(\hat{\mathbf{x}} + i\hat{\mathbf{z}})e^{q_\parallel(ix-z)}. \tag{147}$$

The transverse self-field is circular polarized in every space point. The polarization vector rotates in planes perpendicular to the y direction ($\hat{\mathbf{y}}$). From the quantity $\mathrm{Re}\{(\hat{\mathbf{x}} \mp i\hat{\mathbf{z}})\exp(-i\omega t)\}$, it appears that the direction of rotation is opposite in the vacuum and jellium half spaces. The transverse self-field is linked to the electrostatic ($c \to \infty$) part of the SPM dispersion relation, and therefore the transverse self-field is necessarily rotational-free, i.e.,

$$\nabla\times\mathbf{E}_T^{V,\mathrm{SF}}(x,z) = \nabla\times\mathbf{E}_T^{J,\mathrm{SF}}(x,z) = \mathbf{0}. \tag{148}$$

The reader may readily verify that Eq. (148) is correct.

The transverse self-field is related to the transverse part, $\mathbf{J}_T^{\mathrm{SE}}(x,z)$, of the surface (sheet) current density, $\mathbf{I}$. Thus,

$$\mathbf{E}_T^{\mathrm{SF}}(z,x;\omega) = (i\varepsilon_0\omega)^{-1}\mathbf{J}_T^{\mathrm{SE}}(x,z;\omega), \tag{149}$$

as we shall realize in Sec. VIII D.

From the general microscopic relation [39] $\mathbf{J}_T = i\omega\mathbf{P}_T$, it appears that Eq. (149) in a sense is a special case of the bulk plasmariton relation given in Eq. (141).

The inhomogenous wave equation for the transverse vector potential associated to the surface current density, viz.,

$$\left[\frac{\partial^2}{\partial x^2} + \frac{\partial^2}{\partial z^2} + \left(\frac{\omega}{c}\right)^2\right]\mathbf{A}_T(x,z;\omega) = -\mu_0\mathbf{J}_T^{\mathrm{SE}}(x,z;\omega), \tag{150}$$

tells us [based on Eq. (149)] that the field profile given by Eqs. (146) and (147) is the photon source domain profile. Further insight in the plasmariton source-field dynamics is given in Fig. 5.

The retarded part of the SPM field,

$$\mathbf{E}_T^{V,R}(x,z;\omega) = \mathbf{E}_T^V(x,z;\omega) - \mathbf{E}_T^{V,\mathrm{SF}}(x,z;\omega), \tag{151}$$

$$\mathbf{E}_T^{J,R}(x,z;\omega) = \mathbf{E}_T^J(x,z;\omega) - \mathbf{E}_T^{J,\mathrm{SF}}(x,z;\omega), \tag{152}$$

describes the photon field emitted from the surface current density. We shall see in Sec. VIII that there exists an intimate relation between frustrated T-photon emission in photon tunneling and the confined T-photon picture of the SPM. In the covariant description of SPMs, the L and S photons exist (are nonvanishing) in the entire evanescent profile cf. Eqs (29), (30), (35), and (36). A certain combination of these gives one the longitudinal electric field, $\mathbf{E}_L(z)$ [Eq. (38)], the quanta of which have been named near-field photons [37].

C. Nonretarded eigenmode loop

To (i) determine the transverse self-field of a SPM, and thus its tied T-photon cloud, and (ii) obtain the connection to the T photon-dressed picture of the bulk plasmariton quasiparticle, it is convenient to make use of a propagator formalism, in analogy with what has been done in the atomic case.

It appears from Sec. VIII A that the self-field for SPMs necessarily is connected to the nonretarded part of the electromagnetic propagator. The geometry of the part of the problem makes it convenient to use the Weyl expansion of the propagator. In the mixed Fourier domain, the propagator's nonretarded part, $\mathbf{G}^{\mathrm{NR}}(\mathbf{q}_\parallel,\omega;Z)$, is given by

$$\begin{aligned}&\mathbf{G}^{\mathrm{NR}}(\mathbf{q}_\parallel,\omega;Z)\\ &= -q_0^2\delta(Z)\hat{\mathbf{z}}\hat{\mathbf{z}} + \frac{q_\parallel}{2q_0^2}e^{-q_\parallel|Z|}[\hat{\mathbf{z}}\hat{\mathbf{z}} - \hat{\mathbf{q}}_\parallel\hat{\mathbf{q}}_\parallel - i(\hat{\mathbf{q}}_\parallel\hat{\mathbf{z}} + \hat{\mathbf{z}}\hat{\mathbf{q}}_\parallel)\mathrm{sgn}(Z)],\end{aligned} \tag{153}$$

where $Z = z - z'$ and $\hat{\mathbf{q}}_\parallel = \mathbf{q}_\parallel/q_\parallel$. The expression on the right side of Eq. (153) multiplied by $-q_0^2$ can be recognized as the

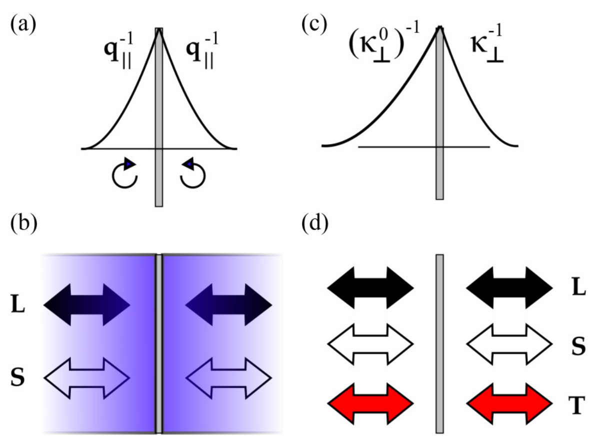

FIG. 5. Graphical representation of the two types of decay length which relates to a T photon tied to a surface plasmariton. (a) The one-dimensional confined source of the T photon has an extension characterized by the decay length $q_{\|}^{-1}$ (the same in vacuum and jellium), and the self-field is circular polarized in opposite directions. As $q_{\|} \to \infty$, one approaches (via the electrostatic region) the geometrical optical limit where essentially complete spatial confinement can be obtained (see Ref. [38], Sec. 5.2). (b) The extension of the T-photon source region (in violet) is in the Coulomb gauge determined by the dynamic Coulomb field extension of the electrons in the current density sheet. In the covariant description, this dynamic field is replaced by the L- and S-photon dynamics (black and white double arrows, respectively). (c) The range of the tied 1D T-photon domain is characterized by the two decay lengths $(\kappa_{\perp}^{0})^{-1}$ (in vacuum) and $\kappa_{\perp}^{-1}$ (in the jellium). (d) As indicated by the three double arrows, a dynamically balanced interaction between the L, S, and T photons in the surface plasmariton state prevents the T photon (red double arrow) from propagating to infinity (be radiated). The double arrow is meant to indicate the dynamic (oscillating) character of the attached energy flows associated to the L, S, and T photons. Compare also to the discussion and arrows related to Fig. 7.

longitudinal part, $\boldsymbol{\delta}_L(\mathbf{q}_{\|};Z)$, of the 2D Dirac delta function tensor, $(\hat{\mathbf{x}}\hat{\mathbf{x}} + \hat{\mathbf{z}}\hat{\mathbf{z}})\delta(Z)$. Hence,

$$\mathbf{G}^{\mathrm{NR}}(\mathbf{q}_{\|}, \omega; Z) = [\equiv \mathbf{G}_{\mathrm{SF}}(\mathbf{q}_{\|}, \omega; Z)] = -q_0^2 \boldsymbol{\delta}_L(\mathbf{q}_{\|}; Z). \quad (154)$$

The small width of the selvedge ($\sim k_F^{-1}$) usually justifies a neglect of the field retardation in propagation across the selvedge, and thus a reduction of the general loop equation for the SPM selvedge field [Eq. (79)] to

$$\mathbf{E}_{\mathrm{SF}}^{\mathrm{SE}}(z) = \int_{\mathrm{SE}} \mathbf{K}_{\mathrm{SF}}(z, z') \cdot \mathbf{E}_{\mathrm{SF}}^{\mathrm{SE}}(z') dz', \quad (155)$$

where

$$\mathbf{K}_{\mathrm{SF}}(z, z') = \frac{1}{i\varepsilon_0 \omega} \int_{\mathrm{SE}} \boldsymbol{\delta}_L(z - z'') \cdot \boldsymbol{\sigma}^{\mathrm{SE}}(z'', z') dz''. \quad (156)$$

As discussed in relation to a study of the field reflection and transmission from a QW selvedge, it is often sufficient to keep only the local part of the self-field propagator [Eq. (78)] in the analyses [see Sec. V D]. The self-field dyad $\mathbf{L} = \hat{\mathbf{z}}\hat{\mathbf{z}}$, entering $\mathbf{g}_{\mathrm{SF}}(z - z') = -q_0^{-2}\delta(z - z')\mathbf{L}$, and its form in other contraction schemes than disk contraction has been discussed in detail in Ref. [39].

D. T photons tied to surface plasmaritons

The selvedge current density $[\mathbf{J}^{\mathrm{SE}}(z)]$ always can be written as a sum of its longitudinal $[\mathbf{J}_L^{\mathrm{SE}}(z)]$ and transverse $[\mathbf{J}_T^{\mathrm{SE}}(z)]$ parts, and for the surface current density in Eq. (27), one obtains in planes outside $z = 0$,

$$\mathbf{J}_L^{\mathrm{SE}}(z) = \boldsymbol{\delta}_L(z) \cdot \mathbf{I}, \quad z \neq 0, \quad (157)$$

and

$$\mathbf{J}_T^{\mathrm{SE}}(z) = \boldsymbol{\delta}_T(z) \cdot \mathbf{I}, \quad z \neq 0, \quad (158)$$

where the sum of the longitudinal ($\boldsymbol{\delta}_L$) and transverse ($\boldsymbol{\delta}_T$) delta functions equals the Dirac delta function times the unit tensor. For $z \neq 0$,

$$\boldsymbol{\delta}_T(z) = -\boldsymbol{\delta}_L(z), \quad (159)$$

implying that

$$\mathbf{J}_T^{\mathrm{SE}}(z) = -\mathbf{J}_L^{\mathrm{SE}}(z), \quad z \neq 0 \quad (160)$$

outside the plasmariton surface current density. The transverse electric field generated by $\mathbf{J}_T^{\mathrm{SE}}$ is given by

$$\mathbf{E}_T(z) = i\mu_0\omega \int_{-\infty}^{\infty} g(z - z')\mathbf{J}_T^{\mathrm{SE}}(z') dz', \quad (161)$$

where $g(z - z')$ is the relevant Huygens propagator in the mixed representation. Two physically equivalent descriptions of the transverse field radiation are shown in graphical form in Fig. 6. In the evanescent part of the $q_{\|}$ spectrum,

$$g(Z) = \frac{1}{2\kappa_{\perp}} e^{-\kappa_{\perp}|Z|} \quad (162)$$

inside the jellium, $\kappa_{\perp}$ being given by Eq. (32). The Huygens propagator in the vacuum half space is obtained with the replacement $\kappa_{\perp} \to \kappa_{\perp}^0$ [Eq. (25)] in Eq. (162).

The transverse electric self-field generated by $\mathbf{J}_T^{\mathrm{SE}}(z)$ is obtained from Eq. (161) letting $c \to \infty$ in the Huygens propagator in Eq. (162). Hence, one obtains

$$\mathbf{E}_T^{\mathrm{SF}}(z) = \frac{i\mu_0\omega}{2q_{\|}} \int_{-\infty}^{\infty} e^{-q_{\|}|z-z'|}\mathbf{J}_T^{\mathrm{SE}}(z') dz' \quad (163)$$

in planes inside the jellium half space. By inserting Eq. (158) into Eq. (163) and carrying out the integration over z', one obtains the result cited in Eq. (149).

Further insight into the inner dynamics of the SPM field can be obtained by studying the associated cycle-average ($\langle \ldots \rangle$) momentum density, given by

$$\begin{aligned} \langle \mathbf{g}(z) \rangle &= \varepsilon_0 \langle \mathbf{E}_T(z) \times \mathbf{B}(z) \rangle \\ &= \varepsilon_0 \big\langle \mathbf{E}_T^R(z) \times \mathbf{B}(z) \big\rangle + \varepsilon_0 \big\langle \mathbf{E}_T^{\mathrm{SF}} \times \mathbf{B}(z) \big\rangle, \end{aligned} \quad (164)$$

where $\mathbf{E}_T^R$ and $\mathbf{E}_T^{\mathrm{SF}}$ are the retarded (R) and self-field (SF) parts of the field; see Eqs. (151) and (152). The magnetic fields in the two half spaces [calculated from $\mathbf{B} = (i\omega)^{-1}\nabla \times \mathbf{E}$] are

$$\mathbf{B}^V(z) = \frac{\hat{\mathbf{y}}}{i\omega}\left(\kappa_{\perp}^0 - \frac{q_{\|}^2}{\kappa_{\perp}^0}\right) A_V e^{\kappa_{\perp}^0 z}, \quad (165)$$

$$\mathbf{B}^J(z) = \frac{\hat{\mathbf{y}}}{i\omega}\left(-\kappa_{\perp} + \frac{q_{\|}^2}{\kappa_{\perp}}\right) A_J e^{-\kappa_{\perp} z}. \quad (166)$$

From Eqs. (10), (11), (165), and (166) (each multiplied by the factor $\exp[i(q_{\|}x - \omega t)]$), a simple calculation shows that

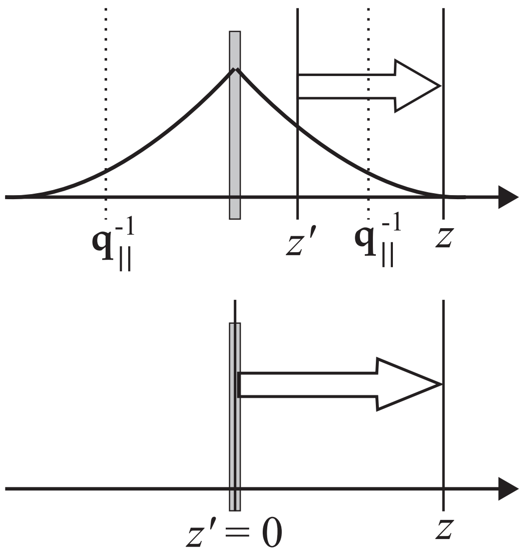

FIG. 6. Graphical representation of the two physically equivalent descriptions of the T-field propagation between source (z') and observation (z) planes. Top figure: With $\mathbf{J}_T^{\mathrm{SE}}(z')$ taken as the source domain (extension given by $q_{\parallel}^{-1}$), *retarded* (with the vacuum speed of light) field propagating connects the z' and z planes, as described by the Huygens scalar propagator. Bottom figure: With the current-density sheet (confined to the plane $z' = 0$), the propagation is described by the dyadic electromagnetic propagator which contains a nonretarded (self-field) part. This part originates in our (mathematical) compression of the source field from $\mathbf{J}_T^{\mathrm{SE}}(z')$ to $\mathbf{I}\delta(z')$. To obtain the field at z, an integration over z' points in the $q_{\parallel}^{-1}$-extended domain is needed in the $\mathbf{J}_T^{\mathrm{SE}}(z')$ picture.

the cycle-averaged z component of the momentum density perpendicular to the surface, i.e.,

$$\hat{\mathbf{z}} \cdot \langle \mathbf{g}(z) \rangle = \frac{\varepsilon_0}{2} \mathrm{Re}[\hat{\mathbf{z}} \cdot \mathbf{E}_T^*(z) \times \mathbf{B}(z)] \tag{167}$$

is zero in every z plane outside the current density sheet, that is,

$$\hat{\mathbf{z}} \cdot \langle \mathbf{g}^V \rangle = \hat{\mathbf{z}} \cdot \langle \mathbf{g}^J \rangle = 0. \tag{168}$$

Not only is the total momentum density flow in the z direction zero, also its retarded and self-field parts vanish for all $z \neq 0$:

$$\hat{\mathbf{z}} \cdot \langle \mathbf{g}^{X,R} \rangle = \hat{\mathbf{z}} \cdot \langle \mathbf{g}^{X,\mathrm{SF}} \rangle = 0, \quad X = V, J. \tag{169}$$

It is obvious that $\langle \mathbf{g}^{X,\mathrm{SF}} \rangle = \mathbf{0}$, and thus also its z component, since there is no magnetic field connected with a self-field (electrostatic field). For the plasmariton, $\mathbf{B}^V(z) = \mathbf{B}^J(z) = \mathbf{0}$ as one sees immediately setting $\kappa_\perp^0 = \kappa_\perp = q_\parallel$ in Eqs. (165) and (166).

In the T-photon language, both the self-field and the retarded T photons are tied in a SPM state. In the Bethe theory for atomic mass renormalization [49], for the propagator description of quantized light emission from an atom [50] and for bulk plasmariton quasiparticles [25], only the transverse self-field is tied to the particle source. The reason for the above difference stems from the fact that the SPM is a *nonradiative (confined) eigenstate* for the particle-field system. In the other cases, one has a *radiative* T-photon part.

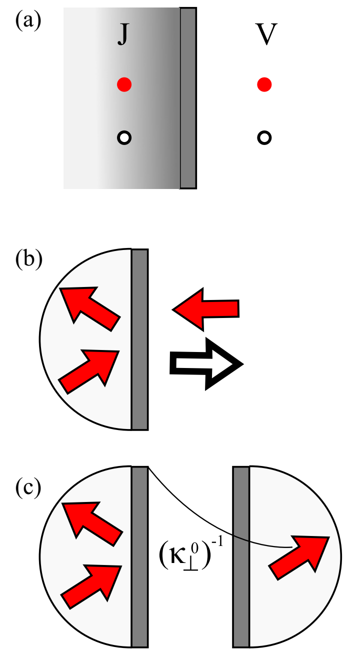

FIG. 7. A graphical representation comparing the momentum energy density pattern perpendicular to the surface in (i) the surface plasmariton state, (ii) total internal reflection (TIR), and (iii) photon tunneling [frustrated total internal reflection (FTIR)]. (a) In the surface plasmariton state, there is no retarded T-photon flow away or toward the source (red dots). The sum of the L and S flows also vanishes (black-white dots). (b) In TIR, the net T-photon flow in the vacuum is balanced by the momentum density flow containing the electric self-field associated with combined L and S photons. (c) In FTIR, the T photon can escape the bound state in the vacuum by inserting a detector (prism) in the $(\kappa_\perp^0)^{-1}$ tail.

Is it possible to release the tied retarded photon part in a SPM? Strictly speaking no, but in T-photon tunneling, where the p-polarized amplitude reflection coefficient $r_p(q_\parallel, \omega)$ plays an important role, the SPM dispersion appears as a pole in the denominator of $r_p(q_\parallel, \omega)$. Briefly speaking, this is so because a SPM is a state with reflected and transmitted field components *without* an incident field. Although $\hat{\mathbf{z}} \cdot \langle \mathbf{g}^V \rangle = 0$, in a reflection process with $q_\parallel > \omega/c$, the retarded and self-field momentum flows are not zero, but [26]

$$\hat{\mathbf{z}} \cdot \langle \mathbf{g}^{V,\mathrm{SF}} \rangle = -\hat{\mathbf{z}} \cdot \langle \mathbf{g}^{V,R} \rangle \quad (>0). \tag{170}$$

Roughly speaking, one may say, on the basis of Eq. (170), that the retarded T photons are pulled back toward the surface plane due to the fact that they never come outside the transverse self-field current density domain, $\mathbf{J}_T^{\mathrm{SF}}(z)$. In photon tunneling between, say two prisms, a tied retarded T photon may be released from the tail of the photon amplitude probability distribution from the source prism once this tail overlaps a detector prism's surface. A schematic illustration of the relation between retarded T-photon tunneling and the SPM state is shown in Fig. 7.

IX. REMARKS ON THE SURFACE PLASMARITON INTERACTION WITH AN EXTERNAL GAUGE FIELD

The SPM with active boundary conditions has the status of an eigenmode of the electromagnetic field, and as such it is nonobservable. This means that one has to seek an excitation of the SPM by an impressed external electromagnetic field. The external field is an impressed field with a prescribed time evolution determined alone by the current density dynamics in the source. If one denotes the contravariant four-potential operator of the external field by $\{\hat{A}^{\mu}_{\rm ext}\}$, the μ component of the symmetrized contravariant current density operator is given as

$$\hat{J}^{\mu}(\mathbf{r},t) = \frac{e}{2m}\sum_{e}\big[\big(\hat{p}^{\mu} - e\hat{A}^{\mu} - e\hat{A}^{\mu}_{\rm ext}\big)\delta(\mathbf{r}-\mathbf{r}_e) + \delta(\mathbf{r}-\mathbf{r}_e)\big(\hat{p}^{\mu} - e\hat{A}^{\mu} - e\hat{A}^{\mu}_{\rm ext}\big)\big], \tag{171}$$

where $\mathbf{r}_e$ is the electron position operator in the $\mathbf{r}$ representation. The electron charge and mass are denoted by $[e(<0)]$ and m, respectively.

In the presence of an external field, the Heisenberg equation of motion keeps the same form as in Eq. (65), yet with the current density operator component $\hat{J}^{\mu}(\mathbf{r},t)$ given by Eq. (171). The impressed external field can only influence the time evolution of the dynamic quantized four-potential through the particle current density.

Since the dynamical equation for $\{\hat{A}^{\mu}(\mathbf{Q};t)\}$ relates to the SPM eigenmode for $\{\hat{A}^{\mu}_{\rm ext}(\mathbf{r},t)\} = 0$, it appears that the set of equations (65), (66), and (171) *cannot* in any way lead to an *exact excitation* of SPM eigenmodes, as is well-known in the classical theory. While passive boundary conditions often can be used in the classical approach, an active surface (layer) is indispensable in the field-quantized description.

In the field-unquantized approach total internal reflection (TIR) of an external incoming field at a dielectric-to-vacuum interface stands as a paradigm for SPM excitation. A covariant photon wave mechanical description of the TIR process was published in Ref. [26]. It appears from this work that in case of a spatially nondispersive dielectric medium (relative dielectric constant $\varepsilon(\omega)$, as in this paper), the whole process reduces to that of an active current density sheet [38].

A calculation of the p-polarized amplitude reflection coefficient, $r_p(q_\parallel,\omega)$ gives the result

$$r_p(q_\parallel,\omega) = \frac{q_\perp^0\varepsilon_{\rm eff}(q_\parallel,\omega) - q_\perp}{q_\perp^0\varepsilon_{\rm eff}(q_\parallel,\omega) + q_\perp}, \tag{172}$$

where $\varepsilon_{\rm eff}$ is the effective dielectric function introduced in Eq. (94). It appears that the denominator in Eq. (172) becomes zero when the SPM dispersion relation is satisfied; see Eq. (93). The plasmariton eigenmode condition thus appears as a resonance in $r_p(q_\parallel,\omega)$; a well-known result in the case of a passive boundary. The condition $r_p(q_\parallel,\omega)\to\infty$ physically corresponds to the situation where one has reflected and transmitted field components without having an incident field. Since both field components are evanescent, this is precisely the SPM eigenmode with an active boundary.

X. PERSPECTIVES

A. The covariant theory in a broader framework

In nonrelativistic quantum electrodynamics, the Coulomb gauge most often is used in dynamical studies of atoms and molecules [32]. The Coulomb gauge, which has the advantage of simplicity, explicitly yields the often predominant Coulomb interaction between particles. This usually is convenient for studies of bound states of charged particles. Although the Coulomb gauge approach *does not* change the fundamental nature of the field-matter interaction, it has the disadvantage of not retaining *manifest* covariance of the field in relativistic QED. In studies on (larger) molecules, it is often necessary to employ a multipole expansion of the field-particle interactions. In such cases, it is often preferable to replace the Coulomb gauge formulation by the Power-Zinau-Wolley approach [51–53], a relative to the Poincare gauge [32].

In QED studies of collective charged particle modes bound near interfaces and surfaces, evanescent mode quantization was opened a little by the Carniglia and Mandel paper [27] on *triplet mode* quantization used in studies of TIR from a flat surface [$q_\parallel > n(\omega)\omega/c$; $n(\omega)$ refractive index without spatial dispersion]. Although the Carniglia and Mandel work does not provide a covariant formalism, the paper was of valuable inspiration for the later Keller and Olesen article [26], giving a manifest covariant photon wave-mechanical description of evanescent fields, quite easily extended to the QED level. As discussed in Sec. VIII D, the covariant formulation allows one to establish a link between the SPM state, total internal reflection analysis, and T-photon tunneling.

In near-field electrodynamics, the covariant formalism can be used in an effective (and economic) manner, carrying out an extra gauge transformation *within* the Lorenz gauge. Thus, a unitary transformation [37]

$$\hat{a}_{\rm NF}(\mathbf{q};t) = \frac{i}{\sqrt{2}}(\hat{a}_L(\mathbf{q};t) - \hat{a}_S(\mathbf{q};t)), \tag{173}$$

$$\hat{a}_G(\mathbf{q};t) = \frac{1}{\sqrt{2}}(\hat{a}_L(\mathbf{q};t) + \hat{a}_S(\mathbf{q};t)) \tag{174}$$

of the annihilation operators for longitudinal (L) and scalar (S) photons leads to two new photon types, viz., a near-field photon and a gauge (G) photon. The associated annihilation operators are denoted by $\hat{a}_{\rm NF}(\mathbf{q};t)$ and $\hat{a}_G(\mathbf{q};t)$. The gauge photon can be eliminated by a suitable gauge transformation within the Lorenz gauge as already mentioned, leaving us with the near-field photon, which, as the word indicates, plays a (prominent) role in near-field QED. The near-field photon, as well as the longitudinal and scalar photons are of importance only when the field-matter interaction is present. These photon types are therefore often called virtual photons. The near-field photon vanishes outside the near-field zone, and the net physical effect of the L and S photons is zero in the absence of field-matter interaction.

The covariant theories of near-field electrodynamics has a meeting point in the electrodynamic near-field interaction of a microscopic near-field probe (atom, molecule, cluster,...) with the plasmariton (and plasmon) spectra of a flat surface.

B. Possible applications of the covariant surface plasmariton theory

1. Möbius band

In the wake of a recently established field-unquantized theory describing the microscopic linear electrodynamics of a Möbius wire [54], it has turned out that also a theory for the electrodynamics of an infinitely thin Möbius band can be formulated. Elements of this theory come out of a general theory for the electrodynamics of curved jellium surfaces in the limit where the Gaussian curvature is identically zero [55]. The general theory is based on a combination of the 2D Schrödinger equation (with the appropriate kinetic energy operator proportional to the Beltrami-Laplace operator, and with an added so-called geometrical potential) and the microscopic Maxwell equations (in the potential formulation with an important term proportional to the Ricci tensor (a certain contraction of the Riemann curvature tensor). The infinitely thin band can carry a dynamic surface current density, and if the length of the Möbius band is much larger than the characteristic wavelength(s) of the electromagnetic field prevailing at the surface, the Möbius band is locally flat, and this allows one to apply the SPM theory with an active boundary described in this paper locally. Gluing together the flat neighboring elements with their slightly changed surface normal vectors, it seems in reach to establish the global eigenmode condition for SPMs on a Möbius band. Initial steps of this program are in progress, and we hope to report on our findings before long.

2. T photon in a cavity

In a matter-free closed cavity, the zero-point fluctuations of the electromagnetic field may play an important physical role. Since field-matter interaction is always present, the cavity eigenmodes cannot be determined in a rigorous sense without including the field-matter interaction in the cavity wall. This interaction involves the exchange of T, L, and S photons. For a metal cavity, the interaction takes place mainly in the surface region (macroscopically characterized by a characteristic field penetration length). Part of the surface interaction is embedded in SPM states. The prevailing surface current density gives the boundary condition for the T-photon field inside the cavity. On the basis of the Ewald-Oseen extinction theorem, the SPMs and plasmons roles can be elucidated [55].

The cavity eigenmodes are unobservable, and thus one must open the cavity in one way or another to apply a prescribed external excitation. In atomic physics, an excited atom propagating through the cavity may change its lifetime due to interaction with the cavity field. The role of the SPMs in this interaction has, to the best of our knowledge, not been studied on the QED level yet.

The importance of the SPMs in a cavity perhaps can be elucidated, making a mesoscopic hole in the cavity. It is known that the diffraction from a mesoscopic hole in a flat screen can give microscopic information on the quantum state of the incoming field (here the cavity field is the incident field). The transmitted field through the mesoscopic hole is what couples to the detector. In an improved version, one may make use of Young diffraction from two mesoscopic holes. A QED theory for Young diffraction from two such holes has been published recently [56].

TABLE I. Overview of the QED approach used in our trio of papers.

P SP	PM	SPM
Scalar K-G[a]	Vectorial K-G	$T1$, $T2$, L, S
Lagrange-Hamilton formalism[b]		Heisenberg Eq. $\{\hat{a}^{\mu}\}$
Minimal coupling principle: Gauge field interaction		
In $\mathcal{L}_P$		In $\{j^{\mu}\}$

[a]The scalar Klein-Gordon equation is only formerly covariant.
[b]An alternative approach for PM in which the displacement field multiplied by (-1) acts as canonical field momentum has also been presented in Ref. [25].

3. Accelerating jellium

In recent years, some attention has been given to the interaction (in Minkowski space) of uniformly accelerating solids with semiclassical and quantum fields, particularly with regard to the thermal Unruh effect [57,58] playing a prominent role in curved space-time. For instance, it is of fundamental interest to understand how a uniformly accelerated jellium interacts with injected charged particles. Such an understanding, obtained via electromagnetic reflection from the jellium, we believe may give valuable information on the microscopic physics of quantized SPMs, possible by extending a photon wave-mechanical theory to the QED level. Some information on the SPM and surface plasmon dispersion relations with passive boundary conditions can be obtained studying the electromagnetic surface dressing of an electron moving uniformly parallel to the jellium surface [59].

C. Comparison of plasmon and plasmariton quantum physics

Recently, in two papers we established photon wave-mechanical and QED theories of bulk and surface plasmons [24] and of bulk plasmaritons [25]. Together with the present paper, our trio of works form a faceted description of the eigenmodes of collective jellium excitations coupled to T, L, and S photons, and their coupling to externally impressed (and prescribed) electromagnetic fields. In Table I, key elements of the trio of papers are listed, using the following abbreviations: P (bulk plasmon), SP (surface plasmon), PM (bulk plasmariton), and SPM. The QED theories for P and SP are based on a scalar Klein-Gordon (K-G) equation which is only formerly covariant since the characteristic phase velocity is $a = \sqrt{3/5}v_F$ (v_F: Fermi velocity of jellium electron sea) and not the vacuum speed of light. Since the plasmariton theory (PM) involves attached photons, it turns out that the vectorial K-G equation is covariant in the rigorous sense. The QED theory for SPM is formulated in terms of a covariant four-photon ($T1$, $T2$, L, S) description, particularly convenient for evanescent mode quantization of p-polarized dynamics. For P, SP, and PM, the quantization is based on the Lagrange-Hamilton formalism. For SPM, the fundamental QED approach is based on the Heisenberg equations of motion for the covariant set of annihilation operators, $\{\hat{a}^{\mu}\}$. The interaction with a prevailing (or external) gauge field is in all cases based on the minimal

TABLE II. Dielectric function entering the P, SP, PM, SPM eigenmodes.† indicates that the spatial dispersion in $\varepsilon_{\text{eff}}(q_\parallel, \omega)$ is associated with the selvedge, the dynamics of which is calculated with neglect of field retardation across the selvedge profile.

P	SP	PM	SPM
$\varepsilon_L(q, \omega)$	$\varepsilon_L(q_\parallel, \omega)$	$\varepsilon_T(q, \omega)$	$^\dagger\varepsilon_{\text{eff}}(q_\parallel, \omega)$

coupling principle (substitution); Lagrangian density ($\mathcal{L}_P$) for P, SP, and PM, and four-current density ($\{j^\mu\}$) for SPM.

The P and SP eigenmode conditions are given by $\varepsilon_L(q, \omega) = 0$ and $\varepsilon_L(q_\parallel, \omega) = -1$, respectively. The PM eigenmode condition is given by $\varepsilon_T(q, \omega) = (cq/\omega)^2$, and at long wavelengths the spatial dispersion usually is negligible, $\varepsilon_T(q, \omega) \simeq \varepsilon_T(\omega)$. For SPM, the effective dielectric function $\varepsilon_{\text{eff}}(q_\parallel, \omega)$ is given in Eq. (94), and its spatial dispersion stems from the constitutive relation associated with the selvedge (surface) current density; see also Table II.

XI. SUMMARY

A SPM is an ideal self-sustained dynamical (lossless) electrodynamical eigenmode requiring an active electron-photon interaction. As such, a SPM always *must* carry a surface current, which, with some justice, most often can be treated as an electric dipole delta function sheet. In the sheet approximation, the electron dynamics is accounted for in the form of a set of jump (boundary) conditions for the electromagnetic field. In Sec. II, we showed that use of the standard (textbook) boundary conditions, in general, is wrong (insufficient) for the SPM eigenmode analysis. Afterward, we established a correct set of what we call active boundary conditions.

From a fundamental quantum physical point of view, the SPM sheet model in this case can be obtained from an adequate reduction of the local-field electrodynamics in the selvedge region. In Sec. VI, we studied the microscopic electrodynamic conditions for reaching the sheet model approximation, and we derived the related SPM dispersion relation for general active boundary conditions.

Most often, nonrelativistic quantum electrodynamic studies are carried out in the Coulomb gauge. In this gauge, the extension of the current density domain of SPMs must be identified with that of the transverse part of a delta function sheet. Since the selvedge dynamics is closely related to near-field electrodynamics, it often is preferable to utilize microscopic local-field analyses on a manifest covariant Lorenz gauge approach. In Secs. III and IV, our wave mechanical theory of SPMs was established using the four-potential connection to the T, L, and S photons. These photon types are coupled via the self-consistently determined sheet current density. In Sec. V, our second-quantized theory of SPMs was developed, starting from the Heisenberg equations for the photon four-potential annihilation operators and the covariant Lorenz gauge.

In Sec. VII, we derived microscopic dispersion relations for the SPMs, modeling the selvedge as a QW. The key quantity in the calculation is the microscopic conductivity tensor, as this appears in the ED limit. Numerical results were presented for one- and two-level QWs assumed to be dominated by diamagnetic and paramagnetic couplings, respectively.

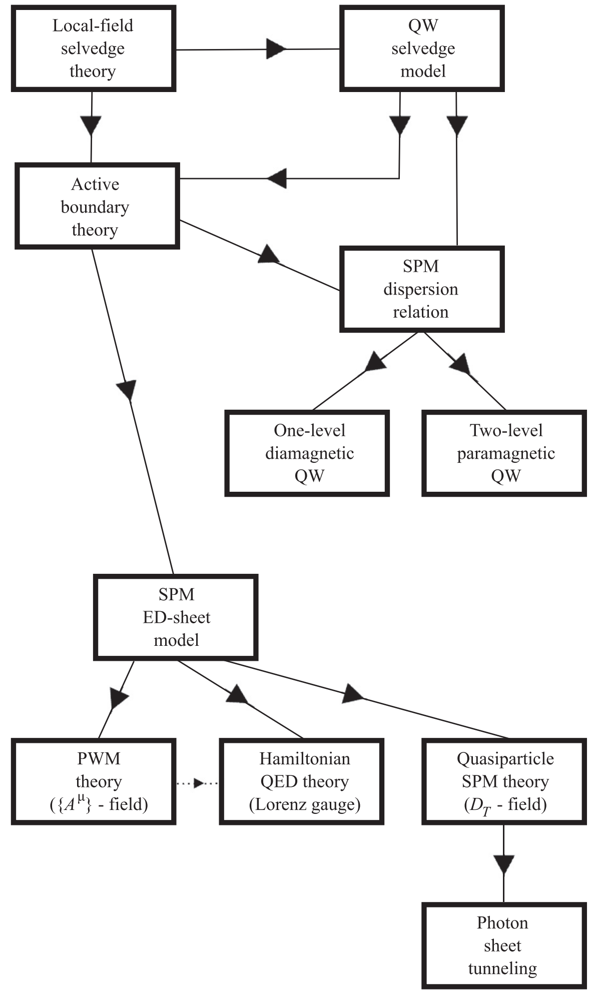

FIG. 8. Schematic diagram showing the connections between central fragments of our SPM theory. Photon wave mechanics abbreviated PWM. The dotted arrow indicates the Heisenberg equation extension from PWM to QED.

In Sec. VIII, we showed that the inner dynamics of a SPM can be understood using a Hamiltonian quasiparticle picture, which is an extension of our quasiparticle theory for PM's. In particular, we showed that the evanescent field of the SPM is associated to the counterpropagating and balanced momentum flows associated to the retarded and self-field parts of the transverse electric field. Thus, outgoing T photons originating in the sheet current density distribution are pulled back toward the sheet and kept in a tied state. In Sec. IX, we showed that this mechanism is frustrated in p-polarized photon tunneling experiments between, say, two parallel-oriented ED current density sheets. It is argued that a physically nice quasiparticle picture of p-polarized photon tunneling appears if this is considered as a frustrated (incomplete) backcoupling of T photons of a SPM. The frustration by the introduction of a second (detector) sheet allows an escape of the T photon from its tied (backcoupled) state.

In Fig. 8, the connections between key parts of our microscopic SPM theory are shown in schematic form.

APPENDIX: COMPARISON TO HYDRODYNAMIC SURFACE PLASMARITON DISPERSION RELATION

Within the framework of the hydrodynamic model, a SPM dispersion relation formally in the form presented in the present paper has been given Moreau *et al.* in Ref. [60] and Pitelet *et al.* in Ref. [61]. For the jellium case, their dispersion relation reads (in our notation)

$$q_\perp + \varepsilon(\omega) q_\perp^0 - i\varepsilon(\omega)\Omega = 0, \tag{A1}$$

where Ω is a quantity related to the spatial nonlocality in the surface density profile. In Refs. [60,61], the electron current density ($\mathbf{J}$), and the electric field ($\mathbf{E}$) are in the frequency domain, and with neglect of irreversible relaxation mechanisms (as in our paper) related by the standard expression (see, e.g., Ref. [11]):

$$\omega^2 \mathbf{J} = \beta^2 \nabla(\nabla \cdot \mathbf{J}) - i\varepsilon_0 \omega_p^2 \mathbf{E}. \tag{A2}$$

Equation (A2) originates in the classical Boltzmann transport equation for the particle velocity, i.e.,

$$m\left[\frac{\partial}{\partial t} + (\mathbf{v}\cdot\nabla)\right]\mathbf{v} = -e(\mathbf{E} + \mathbf{v}\times\mathbf{B}) - m\nu\mathbf{v} - \frac{m\beta^2}{n}\nabla n. \tag{A3}$$

The first moment of Eq. (A3) [with relaxation frequency (ν) and magnetic field ($\mathbf{B}$) both equal to zero] and linearization lead to Eq. (A2). The parameter β usually is taken from a quantum calculation based on the density functional formalism in some approximation. Often, the approximate value $\beta = \sqrt{3/5}v_F$ is used. In our quantum theory of bulk plasmaritons [55], a detailed discussion of the Lindhard RPA theory [44] and the Boltzmann transport equation is given. In Refs. [60,61], one obtains in the jellium case

$$\Omega = \frac{q_\perp}{K^2}, \tag{A4}$$

where

$$K^2 = q_\perp^2 + \left(\frac{\omega_p}{\beta}\right)^2 \frac{1}{\chi_f}, \tag{A5}$$

$\chi_f = -\omega_p^2/(\omega^2 + i\nu\omega)$ being the free (f) electron susceptibility. For $\nu = 0$, $\Omega = q_\perp/[q_\perp^2 - (\omega/\beta)^2]$. In a sense, the calculation of Ω is based on a *spatially dispersive bulk model* (L mode included) extended to space-dependent density variations in the surface profile. In our model, there is no spatial dispersion in the bulk jellium [$\varepsilon(\mathbf{q},\omega) \to \varepsilon(\omega)$]. The active surface current density arises solely from a calculation of the mean value of the microscopic conductivity tensor over the selvedge. This gives a *general* SPM dispersion relation with

$$\Omega = \frac{iq_\perp^0}{\varepsilon_0\varepsilon(\omega)\omega}\left[\varepsilon(\omega)q_\parallel\left(S_{zx} + \frac{q_\parallel}{q_\perp^0}S_{zz}\right) + q_\perp\left(S_{xx} + \frac{q_\parallel}{q_\perp^0}S_{xz}\right)\right], \tag{A6}$$

a quantum result beyond the scope of the hydrodynamic model. In fact, in deriving the result for Ω is was assumed that E_x is continuous at the interface (ABCs for the semiclassical infinite barrier model). Perhaps, the closest one can come to the result of Refs. [60,61] at the low frequencies studied therein is with the diamagnetic QW model. This model has $J_z = 0$ at the surface. From Eq. (125), our microscopic dispersion relation gives

$$\Omega = -\frac{\alpha q_\perp q_\perp^0}{\varepsilon_0\varepsilon(\omega)\omega^2} \tag{A7}$$

and then

$$K^{-2} = -\frac{\alpha q_\perp^0}{\varepsilon_0\varepsilon(\omega)\omega^2}, \tag{A8}$$

where α is the quantum parameter, given in Eq. (123). Note that our K^{-2} is independent of $q_\perp$, thus simplifying the dispersion relation in comparison to that of Refs. [60,61], which give a third-degree equation in $q_\perp$. In fact, a hydrodynamic dispersion relation with spatial dispersion [and quantum parameter $\beta^2 = (3/5)v_F^2$] has been studied many years ago [62], and the solutions to the resulting third-degree equation in $q_\perp$ calculated numerically for (Al).

[1] J. Zenneck, Ann. Phys. **328**, 846 (1907).
[2] A. Sommerfeld, Ann. Phys. **333**, 665 (1909).
[3] A. Sommerfeld, Ann. Phys. **386**, 1135 (1926).
[4] H. V. Hörschelmann, Jb. drahtl. Telegr. u. Telepb **5**, 14 (1911).
[5] H. V. Hörschelmann, Jb. drahtl. Telegr. u. Telepb **5**, 188 (1911).
[6] A. Otto, Z. Phys. **216**, 398 (1968).
[7] E. Kretschmann, Z. Phys. **241**, 313 (1971).
[8] H. Raether, Phys. Thin Films **9**, 145 (1977).
[9] H. Raether, Surf. Sci. **140**, 31 (1984).
[10] H. Raether, *Surface Plasmons on Smooth and Rough Surfaces and on Gratings*, Springer Tracts in Modern Physics, Vol. 11 (Springer, Berlin, 1988).
[11] *Electromagnetic Surface Modes*, edited by A. D. Boardman (Wiley and Sons, Chichester, 1982).
[12] *Surface Polaritons, Electromagnetic Waves at Surface and Interfaces*, edited by W. M. Agranovich and D. L. Mills (North-Holland, Amsterdam, 1982).
[13] *Surface Excitations*, edited by W. M. Agranovich and R. Loudon (North-Holland, Amsterdam, 1984).
[14] W. L. Barnes, A. Dereux, and T. W. Ebbesen, Nature (London) **424**, 824 (2003).
[15] F. Lopez-Tejeira, S. G. Rodrigo, L. Martin-Moreno, F. J. Garcia-Vidal, E. Devaux, T. W. Ebbesen, J. R. Krenn, I. P. Radko, S. I. Bozhevolnyi, M. U. Gonzalez, J. C. Weeber, and A. Dereux, Nat. Phys. **3**, 324 (2007).
[16] S. A. Maier, *Plasmonics: Fundamentals and Applications* (Springer, New York, 2007).
[17] D. K. Gramotnev and S. I. Bozhevolnyi, Nat. Photonics **4**, 83 (2010).

[18] M. S. Tame, K. R. McEnery, S. K. Ozdemir, J. Lee, S. A. Maier, and M. S. Kim, Nat. Phys. **9**, 329 (2013).
[19] S. I. Bozhevolnyi and N. A. Mortensen, Nanophot. **6**, 1185 (2017).
[20] S. I. Bozhevolnyi, L. Martin-Moreno, and F. J. Garcia-Vidal, *Quantum Plasmonics* (Springer, New York, 2017).
[21] N. A. Mortensen, Nanophot. **10**, 2563 (2021).
[22] F. Forstmann and R. R. Gerhardt, *Metal Optics Near the Plasma Frequency*, Springer Tracts in Modern Physics, Vol. 109 (Academic Press, New York, 1983).
[23] P. J. Feibelman, Prog. Surf. Sci. **12**, 287 (1982).
[24] J. Jung and O. Keller, Phys. Rev. A **103**, 063501 (2021).
[25] J. Jung and O. Keller, Phys. Rev. A **104**, 053508 (2021).
[26] O. Keller and D. S. Olesen, Phys. Rev. A **86**, 053818 (2012).
[27] C. K. Carniglia and L. Mandl, Phys. Rev. D **3**, 280 (1971).
[28] H. Raether, *Surface Plasmons—on Smooth and Rough Surfaces and on Gratings*, 1st ed. (Springer-Verlag, Berlin, 1988).
[29] J. D. Jackson, *Classical Electrodynamics*, 3rd ed. (Wiley, New York, 1999).
[30] O. Keller, J. Opt. Soc. Am. B **12**, 987 (1995).
[31] O. Keller, J. Opt. Soc. Am. B **12**, 997 (1995).
[32] C. Cohen-Tannoudji, J. Dupont-Roc, and G. Grynberg, *Photons and Atoms, Introduction to Quantum Electrodynamics* (Wiley, New York, 1989).
[33] L. Lorenz, K. Dan. Vidensk. Selsk. Skr. **1**, 26 (1890); translations in: Ann. Phys (Pogg.) **131**, 293 (1867); and Philos. Mag. **34**, 287 (1867).
[34] F. Mandl and G. Shaw, *Quantum Field Theory*, revised ed. (Wiley, Chichester, 1993).
[35] L. H. Ryder, *Quantum Field Theory* (Cambridge University Press, Cambridge, 1966).
[36] S. Weinberg, *The Quantum Theory of Fields* (Cambridge University Press, New York, 1995), Vol. 1.
[37] O. Keller, Phys. Rev. A **76**, 062110 (2007).
[38] O. Keller, *Light —The Physics of the Photon* (CRC, Taylor & Francis, New York, 2014).
[39] O. Keller, *Quantum Theory of Near-Field Electrodynamics* (Springer, Berlin, 2011).
[40] J. Jung and O. Keller, Phys. Rev. A **90**, 043830 (2014).
[41] O. Keller, Phys. Rev. B **37**, 10588 (1988).
[42] O. Keller, Phys. Rep. **268**, 85 (1996).
[43] A. D. Boardman, in *Electromagnetic Surface Modes*, edited by A. D. Boardman (Wiley and Sons, Chichester, 1982).
[44] J. Lindhard, K. Dan. Vidensk. Selsk. Mat. Fys. Medd. **28**, 8 (1954).
[45] D. V. der Linde, in *Notions and Perspectives of Nonlinear Optics*, edited by O. Keller (World Scientific, London, 1996).
[46] P. Mulser and D. Bauer, *High Power Laser-Matter Interaction* (Springer, Berlin, 2010).
[47] J. Jung and O. Keller, Phys. Rev. A **92**, 012122 (2015).
[48] J. Jung and O. Keller, Phys. Rev. A **98**, 053825 (2018).
[49] H. A. Bethe, Phys. Rev. **66**, 163 (1944).
[50] O. Keller, Phys. Rev. A **58**, 3407 (1998).
[51] E. A. Power and S. Zienau, Philos. Trans. R. Soc. A **251**, 427 (1959).
[52] R. G. Woolley, Proc. R. Soc. London A **321**, 557 (1971).
[53] E. A. Power and T. Thirunamachandran, Am. J. Phys. **46**, 370 (1978).
[54] J. Jung and O. Keller, J. Opt. Soc. Am. B **37**, 3005 (2020).
[55] O. Keller, Fundamentals of Photon Physics (unpublished).
[56] J. Jung and O. Keller, Phys. Rev. A **104**, 013714 (2021).
[57] W. G. Unruh, Phys. Rev. D **10**, 3194 (1974).
[58] W. G. Unruh, Phys. Rev. D **14**, 870 (1976).
[59] O. Keller, Phys. Lett. A **188**, 272 (1994).
[60] A. Moreau, C. Ciracì, and D. R. Smith, Phys. Rev. B **87**, 045401 (2013).
[61] A. Pitelet, N. Schmitt., D. Loukrezis, C. Scheid, H. DeGersem, C. Ciaci, E. Centeno, and A. Moreau, J. Opt. Soc. Am. B **36**, 2989 (2019).
[62] O. Keller and J. H. Pedersen, Proc. SPIE **1029**, 18 (1988).